Tampere University

Miika Vuorenmaa

HIGH-POWER FULL-DUPLEX RADIO PROTOTYPE AT LOWER UHF BAND

RF Self-Interference Canceller Design and Implementation

Master of Science Thesis
Faculty of Information Technology and Communication Sciences
Examiners: Taneli Riihonen, Mikko Heino, Matias Turunen
May 2022

ABSTRACT

Miika Vuorenmaa: High-Power Full-Duplex Radio Prototype at Lower UHF Band — RF Self-Interference Canceller Design and Implementation
Master of Science Thesis
Tampere University
Electrical Engineering – Electronics
May 2022

It has been shown that simultaneous transmission and reception at the same frequency band is possible by cancelling the self-interference (SI) caused by a transmitter. One method for SI cancellation is to couple a low-power sample from the antenna feed and modify this signal to match the received SI signal with an inverse phase, and then combine it with the received signal. The amplitude and the phase of the sampled signal has to be exactly aligned with the received SI signal so that they cancel each other by superposition. Successful cancellation of the SI requires a combination of methods in the electromagnetic antenna domain, in the analog RF front end, and in the digital baseband to enable full-duplex (FD) operation. All of these methods suppress the SI and contribute toward the total cancellation.

Several analog canceller circuits have already been implemented for power levels used in non-military communications and commercial applications. Transmit power level is usually less than 40 dBm (or 10 watts) in these designs. The operating frequency of majority of the cancellers is centered around the 2.4 GHz industrial, scientific and medical (ISM) band and they are implemented using components with low power handling capability. The main challenges for the use of FD radio technology in military communications are to operate at lower frequencies, and to support significantly higher transmission powers from 100 W up to 1 kW. In particular, the power flowing through the components will increase compared to previous analog canceller designs. Therefore, solving these limitations, especially for an analog canceller, is one of the main topics of this thesis and one of the key challenges in the development of high-power full-duplex military radios.

In this thesis, a new high-power analog RF canceller architecture is introduced, which is built on a PCB using discrete power-tolerant components. The new canceller consists of a delay bank in series with a vector modulator and it is designed for the lower UHF band from 225 MHz to 400 MHz which is relevant for military communications. Measurements show that the delay bank combined with the 90-degree adjustable tuning from a vector modulator is able to provide a full 360-degree phase coverage over the entire frequency band. Amplitude tuning range is about 40–50 dB. Cancellation performance is measured over both narrow and wide bandwidths while increasing the input power with different center frequencies from 225 MHz to 400 MHz. The results for a narrow band of 100 kHz show about 30–40 dB of cancellation with maximum available input power. The measurements also study a scenario where a desired signal is received while cancelling the interference. Link budget calculations are performed to estimate possible detection distances for the desired signal while cancelling the interference. The canceller is able to handle 100 watts of transmission power and can be scaled up to 1 kilowatt with slight modifications.

Keywords: full-duplex, analog self-interference canceller, high transmission power, military radios

TIIVISTELMÄ

Miika Vuorenmaa: Suuritehoisen full-duplex radion prototyyppi alemmalla UHF-kaistalla — Itseishäiriön poistopiirin suunnittelu ja toteutus
Diplomityö
Tampereen yliopisto
Sähkötekniikka – Elektroniikka
Toukokuu 2022

Samanaikainen lähetys ja vastaanotto samalla taajuuskaistalla on mahdollista poistamalla lähettimen aiheuttama itseishäiriö. Eräs menetelmä itseishäiriön poistamiseen on kytkeä pienitehoinen näyte lähetysantennin syötöstä ja muokkata tätä signaalia siten, että se vastaa itseishäiriötä vastakkaisessa vaiheessa, jolloin se voidaan yhdistää vastaanotetun signaalin kanssa. Näytteistetun signaalin amplitudin ja vaiheen on oltava täsmälleen kohdakkain vastaanotetun itseishäiriösignaalin kanssa, jotta ne kumoavat toisensa superpositioperiaatteen mukaisesti. itseishäiriön poistaminen mahdollistaa laitteen full-duplex toiminnan ja vaatii osaamista antennien sähkömagneettisessa eristämisessä, analogisessa RF-suunnittelussa ja digitaalissa signaalin käsittelyssä. Jokainen näistä menetelmistä edistää itseishäiriön poistamista.

Aikaisemmin on jo suunniteltu ja rakennettu useita erilaisia analogisia itseishäiriön poistamispiirejä, jotka ovat pääasiassa tarkoitettu pienille alle 40 dBm eli 10 watin lähetystehoille, mikä on yleistä siviiliviestinnässä ja kaupallisissa sovelluksissa. Näillä piireillä on tyypillisesti huono tehonkesto ja ne ovat keskittyneet 2,4 GHz:n ISM-kaistalle *(engl. industrial, scientific and medical)*. Suurin haaste full-duplex-radiotekniikan hyödyntämiselle sotilasviestinnässä on kyky toimia matalilla taajuuksilla ja käyttää huomattavasti suurempia lähetystehoja alkaen 100 watista aina 1 kilowattiin asti. Erityisesti komponenttien läpi menevä teho kasvaa verrattuna aikaisemmin esitettyihin ratkaisuihin. Näiden haasteiden ratkaiseminen, erityisesti analogisen itseishäiriön poistamispiirin suunnittelussa, on yksi tämän diplomityön pääaiheista ja keskeisesti vaikuttaa myös suuritehoisten full-duplex sotilasradioiden kehittämiseen.

Diplomityössä esitellään uusi suurelle lähetysteholle tarkoitettu analoginen itseishäiriön poistamispiirin arkkitehtuuri, joka on rakennettu piirilevylle käyttäen diskreettejä komponentteja, joilla on hyvä tehonkesto. Uusi piiri koostuu viivepankista ja vektorimodulaattorista, jotka ovat sarjassa. Laite on suunniteltu alemmalle UHF-kaistalle: 225–400 MHz, joka on olennainen taajuusalue sotilasviestinnässä. Mittaukset osoittavat, että viivepankki yhdistettynä vektorimodulaattorin 0–90 asteen vaihesäätöön pystyy kattamaan kaikki mahdolliset vaiheet välillä 0–360 astetta koko taajuuskaistalla. Amplitudin säätöalue on noin 40–50 dB. Itseishäiriön poistamiskykyä mitataan koko taajuusalueella sekä kapea- että leveäkaistaisilla signaaleilla samalla kun piirin sisäänmenotehoa kasvatetaan. Suurimmalla käytettävissä olevalla sisäänmenoteholla itseishäiriötä pystytään vaimentamaan noin 30–40 dB kapealla 100 kHz:n kaistalla riippuen keskitaajuudesta. Mittauksissa tarkastellaan myös tilannetta, jossa samanaikaisesti häiritään ja tiedustellaan lähetintä. Linkkibudjettilaskelmien avulla arvioidaan kyseisen lähettimen mahdollista havaitsemisetäisyyttä samalla kun itseishäiriö poistetaan. Suunniteltu piiri kykenee toimimaan 100 watin lähetysteholla ja se voidaan skaalata jopa 1 kilowattiin asti pienillä muutoksilla.

Avainsanat: full-duplex, analoginen itseishäiriön poistaminen, suuri lähetysteho, sotilasradiot

PREFACE

This thesis was done at the Department of Electrical Engineering of the University of Tampere in 2021–2022. The canceller circuit was designed during the spring and summer of 2021. The writing and measurements were done during the fall and winter of 2021. The work was completed in the spring of 2022. The work was funded by the Support Foundation for National Defence (MPKS — Maanpuolustuksen kannatussäätiö), the Academy of Finland, and the Scientific Advisory Board for Defence (MATINE — Maanpuolustuksen tieteellinen neuvottelukunta).

First, I would like to thank Assoc. Prof. Taneli Riihonen for recruiting me into his research group. Especially, his suggestions and supervision helped to carry out this project and to finish it. Secondly, I would like to thank D.Sc. Mikko Heino for his feedback and comments during the writing process and for his help with different simulation softwares. Also, I want to thank, M.Sc. Matias Turunen for his guidance and technical support.

During my work, I was able to develop my skills, especially in RF electronics design. I was able to carry out the design of the electronic device from start to finish, including the design phase, component sourcing, PCB ordering and measuring the operation of the device. I also became more familiar with telecommunications technology and antennas. In addition, I learned to use several measuring devices and design softwares.

A special thanks to my friends for their suggestions. Finally, I want to thank my family for their encouragement and support .

In Tampere, Finland, 23rd May 2022

Miika Vuorenmaa

CONTENTS

1. Introduction 1
2. Full-Duplex and Self-Interference Cancellation 3
2.1 Self-Interference and Cancellation 3
2.2 Passive Self-Interference Cancellation 5
2.3 Active Self-Interference Cancellation 8
2.3.1 Analog Cancellation 9
2.3.2 Digital Cancellation 10
2.4 Defence and Security Applications 11
3. Analog RF Canceller Theory 14
3.1 Analog Cancellation Methods 14
3.2 Proposed Cancellation Approach 16
3.3 Impairments 22
4. RF Canceller Design and Implementation 26
4.1 Overview 26
4.2 Components 27
4.2.1 Protection Switches 28
4.2.2 Delay bank 29
4.2.3 Vector modulator 30
4.2.4 Directional Couplers 33
4.2.5 I/Q Demodulator 34
4.3 PCB Design 35
4.3.1 RF Traces 36
4.3.2 DC Power Supply 39
4.3.3 EMC 40
4.3.4 Power and Thermal Analysis 40
4.3.5 Control Circuit Interface 42
5. Measurements and Results 45
5.1 Measurement Setup 45
5.2 Canceller Parameters 46
5.3 Analog Cancellation Performance 54
6. Conclusion 62
References 64

LIST OF SYMBOLS AND ABBREVIATIONS

AC	alternating current
ADC	analog-to-digital converter
ADS	Advanced Design Systems
AnSIC	analog self-interference cancellation
AWGN	additive white Gaussian noise
BB	baseband
CMOS	complementary metal oxide semiconductor
CW	continuous wave
DAC	digital-to-analog converter
dB	decibel
dBi	decibel isotropic
dBm	decibel-milliwatt
DC	direct current
DiSIC	digital self-interference cancellation
EBD	electrical balanced duplexer
ECAD	electronic computer-aided design
EIRP	effective isotropic radiated power
EM	electromagnetic
EMC	electromagnetic compatibility
EMI	electromagnetic interference
ENIG	electroless nickel immersion gold
FB	feedback
FD	full-duplex
FDD	frequency-division duplexing
FM	frequency modulated
FSPL	free-space path loss
GCPW	grounded coplanar waveguide

GND	ground
HD	half-duplex
IBFD	in-band full-duplex
IC	integrated circuit
IMD	intermodulation distortion
IQ	in-phase and quadrature
LED	light emitting diode
LNA	low noise amplifier
LO	local oscillator
LPF	low pass filter
MFDR	military full-duplex radio
MOSFET	metal-oxide-semiconductor field-effect transistor
NF	noise figure
P1dB	1 dB compression point
PA	power amplifier
PCB	printed circuit board
PLS	physical layer security
QFN	quad-flat no-leads
quasi-TEM	quasi-transverse-electromagnetic
RF	radio frequency
RoHS	restriction of hazardous substances
RX	receiver
SF-STAR	same frequency simultaneous transmission and reception
SI	self-interference
SINR	signal-to-interference-to-noise-ratio
SMA	sub miniature version A connector
SMD	surface mount device
SMT	surface mount technology
SP6T	single-pole six-throw
SP8T	single-pole eight-throw
SPDT	single-pole dual-throw
TAU	Tampere university

TDD	time-division duplexing
THT	through hole technology
TL	transmission line
TX	transmitter
VM	vector modulator
VNA	vector network analyzer
VST	vector signal transceiver
VSWR	voltage standing wave ratio

1. INTRODUCTION

The idea of simultaneous transmission and reception at the same frequency band is not new in radio technology but has not been implemented before because it was believed to be impossible. A transmitting radio causes strong interfering noise to all surrounding receivers that operate on the same or close frequency band, including the radio's own receiver. The receiver is saturated by the strong transmission signal and all of the incoming desired signals are hidden under it. This unwanted interfering noise is called self-interference (SI). The SI has to be suppressed in order to allow the receiver to operate simultaneously with the transmitter.

Simultaneous transmitting and receiving has been already used for a long time in wired networks where parallel cables carry information in both directions. However, in wireless radio communications, information is carried by propagating electromagnetic (EM) waves which share a common medium that cannot be separated. Conventionally, transmit and reception channels are offset in the frequency domain due to the adjacent channel leakage because some portion of the transmission power leaks into the receiver channel. Frequency separation is needed because any practical filter cannot provide an ideal step frequency response as there is always some kind of slope in a filter's transition band. Different type of filters are used to eliminate the unwanted frequencies.

In-band full-duplex (IBFD) describes a system that is able to transmit and receive on the same frequency band at the same time. The self-interference is cancelled by simply subtracting the transmission signal from the received signal. This is possible because the transmission signal is known to the device. Therefore, there is no need for additional filters or frequency offsets. This allows dynamic radio frequency (RF) spectrum usage and sharing.

The purpose of this master thesis is to design and build an analog RF self-interference canceller for a high-power full-duplex radio that operates at the lower UHF band from 225 MHz to 400 MHz which is also known as the NATO band I. This particular frequency band is chosen because it seems to be most appropriate for cognitive military radios. Due to the high transmission power, good isolation between the transmitter and the receiver is required. The purpose is to passively reduce the amount of self-interference in the receiver before applying any analog or digital cancellation. Different isolation techniques

are studied because they affect the analog RF canceller design.

The proposed analog RF canceller design is a new architecture to provide 360 degrees of vector modulation. The RF canceller has a delay bank in series with a vector modulator. The delay bank provides the initial group delay while the vector modulator allows attenuation control and additional phase adjustment from 0 to 90 degrees. Together, they are able to cancel the SI by adjusting the amplitude and phase of the coupled transmission signal. Effective SI cancellation requires that the amplitude of the coupled signal to be equal with an inverse phase. The coupled cancellation signal can be combined with the SI so that they cancel out.

The power passing through the canceller increases with respect to the high transmission power, which introduces more power losses resulting in heat generation and exposes components to non-linearity. Thus, high-power tolerant components are used to allow higher RF input power. However, the input power cannot be increased indefinitely because the maximum power ratings of small integrated circuits (IC), such as RF switches and PIN-diodes, are a limiting factor.

Laboratory measurements confirm that the RF canceller built on a printed circuit board (PCB) provides full 360 degrees of vector modulation and is able to successfully cancel the SI with a high transmission power. The measurements are done at three different frequencies to analyze how the RF canceller operates at the lower, middle and upper end of the band. The SI cancellation performance is studied as the RF input power increases and potential impairments are discussed that affect the operation of the device. Link budget calculations are used to estimate that from how far the incoming signal can still be detected with the analog RF canceller alone.

This thesis is structured as follows: Chapter 2 describes the self-interference phenomenon, studies different methods to cancel it and briefly presents some applications that would benefit from the designed RF canceller. In Chapter 3, previous analog canceller designs are discussed and a new high-power RF canceller architecture for lower UHF is presented. Chapter 4 describes the electrical design process of the RF canceller board, including component choices, PCB structure, design aspects, and provides an interface for a control circuit. Chapter 5 focuses on the measurements and their analysis. Finally, Chapter 6 summarizes the thesis.

2. FULL-DUPLEX AND SELF-INTERFERENCE CANCELLATION

In this chapter, the theory of an in-band full-duplex system is presented. The reasons for self-interference are investigated and distinctive accessible strategies to decrease and suppress the self-interference are shown. The self-interference can be cancelled by numerous diverse techniques and topologies [1, 2], yet the concentration in this work is on designing and building an analog RF canceller board. Other topics, such as digital cancellation, are only overviewed for completeness. In addition, full-duplex applications in defence and security fields are studied as the designed canceller is especially beneficial in such applications.

2.1 Self-Interference and Cancellation

A basic wireless radio system consists of a transmitter (TX) and a receiver (RX). TX and RX communicates with each other using a channel, which can be either a point frequency or a range of frequencies. If a device can operate in both modes, it is called a transceiver. The modern communication systems such as base stations and mobile phones are transceivers. The communication between these devices is bi-directional as they both transmit and receive signals. Traditionally, these devices still operates in half-duplex (HD) or out-of-band full-duplex modes. [3]

Currently, the two most used methods for duplexing are time division duplexing (TDD) and frequency division duplexing (FDD). Time division duplexing divides the operation in the communication channel into TX and RX periods. Frequency division duplexing uses two different channels, one for the TX and another for the RX. [4] By introducing the in-band full-duplex (IBFD) system, the RF spectrum efficiency and capacity can be theoretically doubled [3, 4] because a wireless device is capable of transmitting and receiving data simultaneously at same frequency. This makes IBFD systems superior compared to the TDD and FDD methods in terms of channel usage. However, IBFD is not suitable for all types of wireless communication applications because it excels only in systems with approximately the same amount of transmission and reception. It has also gathered a lot of attention in the industrial and scientific communities [3, 5]. Figure 2.1 presents a comparison between these three methods and demonstrates their the channel usage.

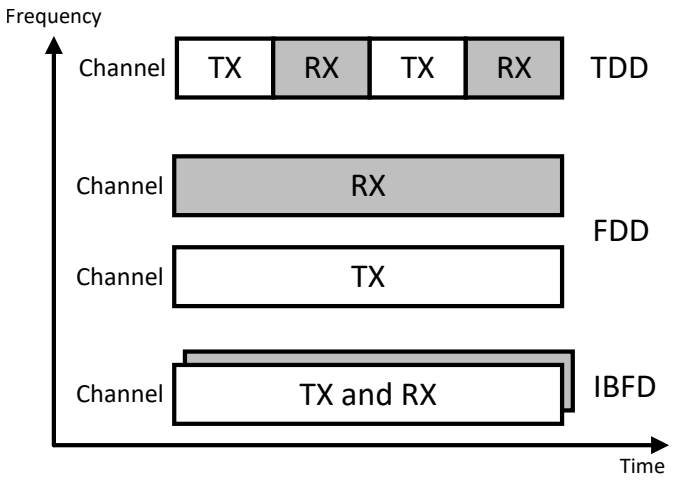

Figure 2.1. *TDD, FDD and IBFB operations compared.*

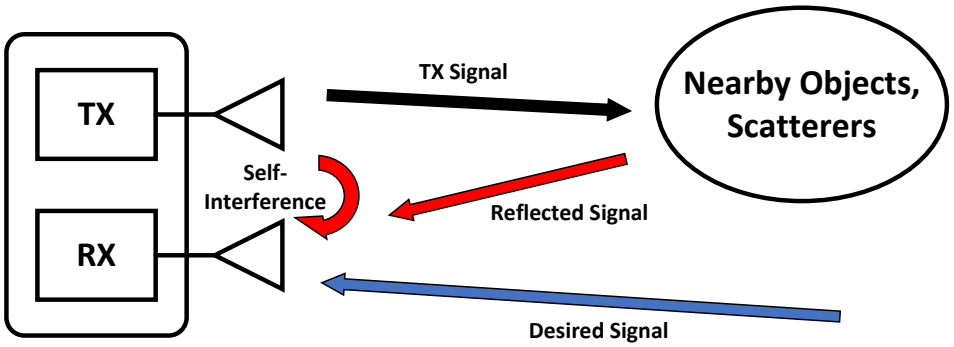

Figure 2.2. *Full duplex in dual antenna configuration.*

The main issue of full-duplex (FD) systems is the self-interference (SI) caused by the device's own transmitter. The SI must be cancelled, otherwise the receiver will be fully saturated and it would be unable to distinguish any other desired signals because they are buried under the strong SI. The effects of the SI cannot be ignored because a system's receiver and transmitter are typically located at the vicinity of each other. In practical systems, the distance between them is significantly shorter than the distance from the other nodes in the area. The desired signals coming from the other nodes will be attenuated due to a path loss which means that the received signal will be few orders of magnitude weaker than the own TX signal. Figure 2.2 shows a basic dual antenna configuration in full-duplex systems. The self-interference has a direct coupling path from TX antenna to RX antenna, also referred as a primary SI path because it is the major source of the SI. The transmitted signal can also be reflected or scattered from nearby objects which creates multiple paths for the self-interference. The reflections usually contain multiple copies of the original signal with various amplitudes and phases which makes the cancellation process more complex. These multi-path components are referred as a secondary paths for the SI. [3, 6]

RF cancellation process starts with the passive SI cancellation which attenuates the SI on the coupling path. Then, the leakages are further decreased by active cancellation consisting of an analog RF canceller circuit and a digital canceller. Digital cancellation is applied after SI is sufficiently removed in the analog domain and the signal is in the dynamic range of the analog-to-digital converter (ADC) [1, 3]. The major challenge is the analog canceller circuit design and optimization. In order to achieve maximum SI suppression, the RF canceller system implementation must use a combination of passive and active cancellation methods. The objective is to cancel the SI to the receiver's noise floor.

2.2 Passive Self-Interference Cancellation

Passive cancellation techniques suppress the SI signal in the propagation domain. The purpose is to electromagnetically isolate the TX signal from the receiver so the strong SI signal is attenuated before it reaches the RX antenna. Passive cancellation typically tries to minimize the effect of the direct coupling path. Different methods enhance the attenuation by altering or blocking the SI path. [7] It is desired to have maximum amount of isolation between the TX and RX chains because it counts towards total cancellation. This will also decrease the chance that the receiver gets saturated or the signal gets distorted when the TX signal is not fully being cancelled [3].

Typical antenna configurations for a FD system are shared and separated antenna topologies. A shared-antenna system uses a single antenna for both TX and RX . The separated antenna design uses dual antenna configuration where a full-duplex system has one for TX and another for RX. Antenna isolation improvement methods present clever antenna designs and placement for a dual antenna setup [6, 7, 8].

The first method is to increase the physical distance between the two antennas, due to the path-loss, the RX signal will be weaker than the original TX signal. This can be called as the intrinsic isolation caused by the separation. The issue is that the RX and TX antenna terminals are usually part of the same device or the antennas are placed quite close to each other. For example, they could be located at the top of the mast where one is almost right above the another.

The second method is to weaken the propagation of electromagnetic waves between the antennas. This is done by introducing some physical barrier or parasitic elements between the antennas [3]. In the case of physical barrier, the TX signal reaches the RX antenna via reflections or diffraction. One way to decrease the SI is to use cross polarization for isolation where device antenna terminals are aligned so that it uses one polarization for transmitting and different one for receiving.

The third method is to use more complex antenna designs such as antenna arrays which

create a suitable null at the direction or place of the RX antenna [8]. One possibility is to utilize two directive antennas if the radiation pattern specifications allow to do that. Also, TX nodes can be placed in such a way that TX signals are exactly out of phase and cancel each other at the receiver's position [8].

The best isolation solution would be an antenna design that combines all the three methods. For example, constructing a cross-polarized directive antenna with a parasitic decoupling element. This will increase the isolation at the cost of a more complicated antenna design. It is possible to reach about 40–50 dB isolation between the two antennas in practical scenarios as the following studies show [8, 9]. Thus, it is assumed that such amount of antenna isolation is available for the RF canceller system and value can be used in further calculations.

Circulator

A circulator is usually a 3-port electrical device made of ferromagnetic material and used to regulate the signal flow within a circuit [10]. It can be either be a passive or an active component, while the passive ones are much more common. Ideally, the signal cannot propagate to the opposite direction and the third port is being isolated. The circulator transmits the signal in one direction with a small amount of insertion loss [10]. For example, the signal input is port 1, and from there signal is forwarded to port 2, while being isolated from port 3. This principle still applies even though a different input port is chosen. In other words, input at port N will cause output at port $N+1$. Three-port circulator operation is based on cancellation of waves propagating over two different paths close to a magnetized material [10]. Mathematically this function can be expressed with scattering parameters. The scattering parameter matrix for a lossless circulator can be written as

$$S = \begin{bmatrix} \alpha & \gamma & \beta \\ \beta & \alpha & \gamma \\ \gamma & \beta & \alpha \end{bmatrix}, \tag{2.1}$$

where α is the reflection coefficient, γ is the main line insertion loss and β is the isolation.

A circulator can be used as a duplexer which allows sharing a common antenna between the transmitter and the receiver [10]. This property makes it conceivable to have full-duplex operation utilizing only one antenna. The configuration is shown in Figure 2.3. Now, the SI channel is the between the TX and RX ports so the circulator's isolation value determines the passive cancellation.

When choosing a circulator for a FD application, several electrical parameters have to be checked, which are frequency, insertion loss, isolation and power handling. Real components have always some losses and unwanted leakage between ports. Insertion loss is

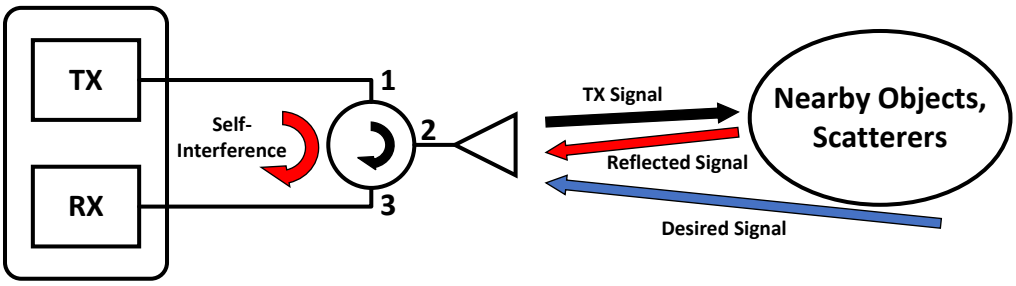

Figure 2.3. *Circulator as duplexer with single antenna configuration.*

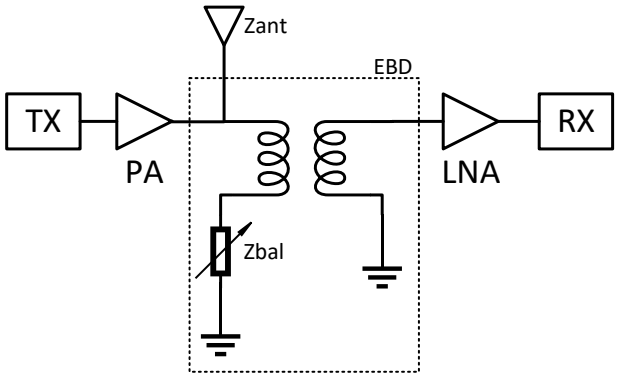

Figure 2.4. *Structure of EBD-based analog SI cancellation setup [11].*

about 0.5 dB in main direction. Isolation is typically about 20–30 dB depending on the circulator type and size [10]. In addition, it should be kept away from other ferrous metals, because they may affect the frequency response of the circulator. The component can be implemented in several different packages with different physical dimensions and mounting techniques. [10]

Electrical Balance Duplexing

The electrical balanced duplexer (EBD) is a hybrid solution as it can be considered either as a passive or an analog SI cancellation solution that has high linearity and low insertion losses. It is an alternative single-antenna method for full-duplex operation [11]. A basic single-ended EBD topology is shown in Figure 2.4. EBD circuit consists of four ports, where the opposite ports are isolated from each other [12]. This configuration requires external devices such as a power amplifier (PA), an antenna and low noise amplifier (LNA), connecter to the EBD's terminals.

This EBD concept is based on the hybrid transformer, which provides signal cancellation through the electrical balancing of the two impedances: Z_{ant} is antenna impedance and Z_{bal} is the virtual load also called as the balancing network, which can be an external

circuit or a part of internal design of EBD IC chip. When a signal enters at one of the ports, it travels to each of the adjacent ports, but due to the different phase of the adjacent ports, the signal at the opposite port is cancelled. Isolation is implemented by adjusting the port impedances such that the signals are exactly in opposite phases [12]. Finding a good balance between these two aforementioned impedances increases the isolation [12]. Usually, EBD is implemented on the chip by using silicon isolator technology, making it suitable for mobile and other wireless platforms. [11]

The EBD circuit requires constant tuning because antenna impedance is frequency and time dependent and it varies with respect to the environment due to changes in the near-field [6, 12]. The balancing network should be adjusted with a high-accuracy adaptive algorithm to match the antenna impedance over the operation frequency range [13]. An optional antenna tuning circuit can be connected between the antenna and EBD terminal [6, 13]. The purpose is to introduce dynamically controlled impedance matching, which reduces the impedance pool seen by the EBD [13].

Mathematically, EBD circuit can be modeled by assuming ideal S-parameters for symmetric hybrid transformer, so the isolation I between the TX and the RX can be calculated in decibels as:

$$I = 20 \log |\Gamma_{ant} - \Gamma_{bal}| - 6.02, \tag{2.2}$$

where Γ_{ant} and Γ_{bal} are the complex reflection coefficients which can be calculated as

$$\Gamma_{ant} = \frac{Z_{ant} - R_O}{Z_{ant} + R_O}, \tag{2.3}$$

where the Z_{ant} is the antenna impedance and R_O is the output load. [11] The impedance balance between Z_{ant} and Z_{bal} is called equilibrium. In the equilibrium, two samples of the transmit signal are induced to the secondary winding of the hybrid transformer. These samples have equal amplitude and are in opposite phases. Thus, this structure could result in infinite direct SI cancellation, at least in theory. [11]

2.3 Active Self-Interference Cancellation

Active SI cancellation can be divided into analog SI cancellation (AnSIC) and digital SI cancellation (DiSIC). Analog cancellation methods provide the SI cancellation in the analog circuit domain before the signal enters the RX chain's ADC. Digital-domain SI cancellation can applied when the SI signal has been suppressed enough in the analog domain. Its purpose is to mitigate the residual SI that is left from the passive and analog cancellation. Together they all count towards the total SI cancellation.

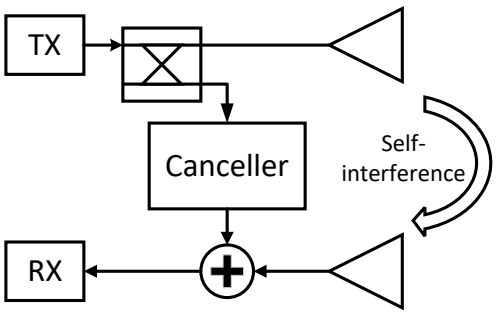

Figure 2.5. *Block diagram of a full-duplex transceiver.*

2.3.1 Analog Cancellation

Analog RF cancellers couple a sample from the transmitter output that is called the cancellation signal. It is a low power copy of the original transmission signal. The SI cancellation is possible because the received SI signal is the device's own transmit signal whose waveform is known. The cancellation is done by adding an equal signal that is 180 degrees out of phase signal with the received SI signal. The analog canceller has to adjust the cancellation signal's amplitude and phase to match the received SI with opposite phase and, finally combine the two signals. Due to wave superposition the SI signal will get cancelled. The basic structure of a FD transceiver with an RF canceller is shown in Figure 2.5.

It is important that the input coupler is placed right before the antenna in TX chain because the antenna feed signal contains the information about the transmitter's non-idealities. The sources for the TX signal's non-idealites could be phase noise, phase drift, power amplifier's non-linearity, etc. These same non-idealities are also seen in the SI signal so their effects would be inherently cancelled. The SI cancellation might seems like an easy task in theory, but it has some practical challenges that can be already noted.

To reach high levels of cancellation, the amplitude must be precisely the same and the phase must be exactly aligned to get the 180-degree phase difference. The phase error is more significant than the amplitude error because having the relative difference in both parameters will cause more decrease in cancellation when applied to the phase. For example, the phase is poorly adjusted and the SI and cancellation signal happen to be in the same phase instead of the opposite phase. This will amplify the SI and increase canceller output power. In practice, there are always some misalignment in the both parameters which is why a perfect cancellation cannot be achieved.

Self-Interference Signal Model

A mathematical model can be used to described the SI signal and the analog cancellation process. Assume that $x(t)$ is a complex-valued baseband TX signal. A sample of this signal is coupled to a canceller input and that is expressed as

$$w(t) = h_c \cdot x(t), \tag{2.4}$$

where h_c is the coupling factor. The SI seen at the RX input can be also modeled as complex valued baseband signal that includes multi-path components where multiple copies of the SI with different amplitudes and phases are reflected back to the RX antenna. This is expressed as

$$y(t) = \sum_{n=1}^{N_{SI}} h_{SI,n} \cdot x(t - \tau_{SI,n}) + n(t), \tag{2.5}$$

where $h_{SI,n}$ is the decoupling coefficient, $\tau_{SI,n}$ is delay of the n-th SI component and $n(t)$ represents thermal noise [14]. The RF canceller circuit can have total of N_c parallel cancellation paths, also known as taps, while it enables adjustable amplitude and phase control for coupled input signal $w(t)$. The SI cancellation process in complex-valued baseband form can be expressed as

$$z(t) = y(t) - h_c \sum_{n=1}^{N_c} w_n \cdot x(t - \tau_{c,n}), \tag{2.6}$$

where w_n is the amplitude and phase control of the n-th cancellation path and $\tau_{c,n}$ is the phase delay of the n-th cancellation path [14, 15]. Each cancellation path has both amplitude and phase control, so the set of delay taps N_c does not need be identical or provide same delay as $\tau_{SI,n}$ of the SI coupled channel. This allows the SI waveform to be reproduced accurately. Similarly, the number of cancellation paths does not have to be the same as the actual number of SI multi-path components [15]. Equation 2.6 can be further simplified if the canceller design has only one tap or channel, where N_c equals to one.

2.3.2 Digital Cancellation

Conventional digital-domain SI cancellation operates similarly to analog cancellation as it also creates a copy of the original TX signal and then by scales and subtracts these copies from the RX signal [16]. A major disadvantage for FD systems that are only based on the digital cancellation is the hardware requirement for the ADC because it would require vast dynamic range in order to acquire and process both high-power self-interference and low-power desired signals [3]. This sets a requirement to apply the analog cancellation prior to digital cancellation, especially in high-power FD systems.

The benefits of digital cancellation are that the sophisticated signal processing methods become relatively simple in digital domain compared to a similar analog circuit where same functionalities are implemented [16]. It is possible to include these to the analog design but the circuit's complexity and power consumption would increase significantly [16]. So it is far more common perform the SI post-processing digitally [3].

Phase noise and non-linearity are two main issues for conventional digital cancellation that limit the performance [16]. Phase noise is short-term frequency instability that is caused by non-ideal local oscillators as their frequency slightly varies in time that creates small side bands around the oscillator's center frequency [17]. The long-term instability is called as frequency drift and its main cause is usually temperature [17]. The other issues are non-linearities in both TX and RX chain due to component and hardware imperfections [16]. If the digital canceller takes its input before the digital-to-analog converter (DAC), the transmit signal changes and even distorts as it passes through the components in the TX chain so the actual SI signal will differ from the original input signal [3, 16]. The same issue is also seen in the RX chain [16].

In order to improve digital cancellation, the digital canceller needs a signal copy from the antenna feed as the analog cancellers do. Thus, digital canceller would be able to cancel out both the SI signal and its related impairments. This can be implemented by adding an auxiliary receiver chain that obtains digital domain input from the antenna feed [16] or from the analog canceller's feedback. However, it only eliminates the transmitter impairments but the receiver chain impairments still apply so it cannot provide perfect SI cancellation [16].

2.4 Defence and Security Applications

In this section, the possible applications of FD technology are discussed. The advantages of FD technology in defense and security applications remain largely unexplored. The high-power canceller would highly benefit these applications, because they operate with high transmit powers.

In-Band Full-Duplex Radar

FD technology is known for its potential to double the spectral efficiency but is not the only benefit of this technology. The multi-path reflections were considered as undesirable in the FD radios as they are hard to predict and makes the SI cancellation more complicated. However, they are now useful because they allow the device to recover the environmental reflections of the transmission. From a radar perspective, the FD radio can be viewed as an integrated radar illuminator and receiver. [11]

There are two types of radar: pulsed and continuous wave (CW) radar systems. The

pulsed radar system operates by switching the transmission on and off, while the TX is off, it waits for the signals to reflect back to the antenna. The continuous wave system could benefit from FD technology if the high-power RF canceller is able to cancel its self-interference which is also known as transmitter leakage. Currently, the SI limits the maximum TX power in CW radars, but with sufficient cancellation, the detection range can be theoretically increased. At the moment, CW radars are used for short-range target detection so is it does not need to shutdown the transmission to receive signal. While pulsed radar systems are used more for a long range detection. [3]

Typical CW radars use similar antenna configurations as those presented in Figures 2.2 and 2.3. A bistatic radar has two separated antennas and the isolation is achieved using separation but the isolation can be further increased by placing magnetic material elements between them. A monostatic radar is typically similar to the circulator design where it uses only single antenna for both TX and RX. So similar isolation methods can be utilized for radars. [3]

Military

In the military perspective, FD technology has both defensive and offensive purposes. IBFD radio's defensive capabilities can be utilized in a situation where the enemy is performing an electronic attack during a friendly transmission. The objective is to detect the attack, such as jamming, and deploy countermeasures. [18] Also, it can be used to gather information about the attack, which can be further used to gain tactical advantage over the enemy. Studies have shown that it is possible to detect presence of an enemy while transmitting on overlapping frequencies even if it uses low jamming power or smart jamming techniques, where the enemy stops the jamming at same moment, when the friendly transmission is over [18, 19, 20].

Offensive use of FD radios focuses on monitoring the radio spectrum for potential enemy transmissions and intercepting their broadcasts by jamming their frequencies. Also, it is used to observe effectiveness of jamming and study how the enemy transmitter behaves. [19, 21] It can increase its TX power, change signal's waveform or switch totally to other communication methods. The FD system is capable of performing these actions simultaneously. Thus, armed forces might gain tactical advantage by conducting electronic attacks and denying enemy's communications or at least hinder them [18, 19].

Almost all military radios today use the traditional time division or frequency division HD transmission for tactical communications [18]. Thus, improvement of spectrum efficiency is also crucial in military networks. In the future, military full-duplex radio (MFDR) will have an unprecedented same-frequency simultaneous transmission and reception (SF-STAR) capability, and it may even provide significant technical advantages in the battlefield [19, 20]. The use of MFDR not only provides the transmission of bidirectional information

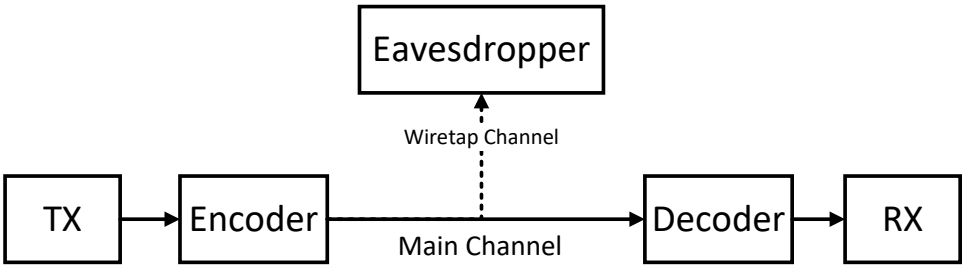

Figure 2.6. *Eavesdropping attack by wiretapping the main TX channel.*

with efficient use of the spectrum, but also allows the armed forces to combine electronic warfare with tactical communications [18, 19]. This will lead to new tactics and systems executing electronic attacks during transmissions.

Physical Layer Security

Physical layer security (PLS), or also known as information theoretic security, is emerging as a potential method to secure communication against eavesdropping attacks by exploiting the characteristics of wireless channels [22]. In the eavesdropping attack an adversary wiretaps into wireless network where the malicious nodes eavesdrop either the transmitter or the receiver. This transmitting network can be modeled as a main broadcast channel with a wiretap channel as shown in Figure 2.6. In order to fully obtain the transmitted information the eavesdropper must be in synchronization with the wireless network. [23, 24] As long as the eavesdropper is unable to decode any of the transmitted bits, it is considered as a perfect privacy [24]. PLS does not require any information or assumptions about the adversaries, that is one of its advantages [23, 25]. The mathematical model for the PLS is based on the Shannon research on the information theoretic security called "perfect secrecy" in the 1940's. Later, Wyner continued the research in his work "weak secrecy" in the 1970's. [22]

IBFD radios can utilized to secure the wireless communications by transmitting noise on the channel while receiving a secret key from another node. The legitimate receiver can decode the secret key by cancelling the interference. However, the eavesdropper is unable to receive the secret key because it is hidden under the transmitted interference. [22]

PLS differs from conventional cryptography as the achieved security at the physical layer is unbreakable even if the adversary has an infinite amount of computational power available. Interest towards PLS has risen since the threat of decrypting the current key agreements. This threat is posed by the development of quantum computers. [22] PLS can be also used to enhance existing cryptographic schemes [23, 25].

3. ANALOG RF CANCELLER THEORY

In this chapter, theoretical modeling and practical designs of an analog canceller are studied. A new canceller implementation for high transmit power and low frequency is presented and compared with other approaches in the most recent research papers. Also, the advantages and impairments of such system are being analyzed.

3.1 Analog Cancellation Methods

A full 360-degree vector modulation is the most important aspect of the RF canceller circuit because it should have the ability to control both amplitude and phase of the coupled signal for the whole operating frequency band. The amplitude and phase tuning must be accurate as the amplitude has to be exactly the same and out of phase in order to effectively cancel the SI when combined with the received signal. However, the multi-path components of SI signal are problematic for the cancellation. Therefore, several canceller circuits have more than one tap in their design. One tap canceller structure is suitable for a narrowband cancellation and is able to cancel the strongest SI component which is usually caused by the direct coupling path. Multi-tap solutions are also able to cancel multi-path components caused by SI reflections. Typically, there is some phase difference between the different taps. Each tap has at least its own amplitude control and in some cases also phase control is included. Multi-tap cancellers are suitable for broadband cancellation.

Many previously developed RF cancellers have been shown to successfully attenuate SI, but they are designed for power levels below 40 dBm with low- power handling capability. These circuits are typically designed for carrier frequencies over 1 GHz. [5, 22]. Thus, they would not be sufficient to support the military frequency bands and power levels. For example, research institutes such as MIT and Stanford have presented their analog RF canceller designs. These cancellers have been successful for 2.4–2.5 GHz region with the maximum bandwidth of 100 MHz [26, 27] so analyzing their design principles may give some insights for developing an RF canceller for high power and low frequency. In addition to MIT and Stanford cancellers, similar research has also been done elsewhere, such as at RICE University in Houston, Texas [28, 29].

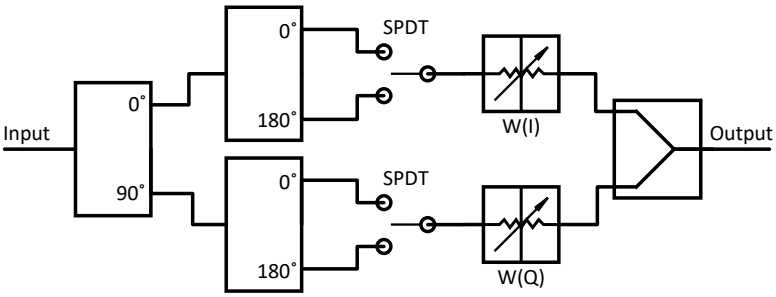

Figure 3.1. *MIT analog canceller design [26].*

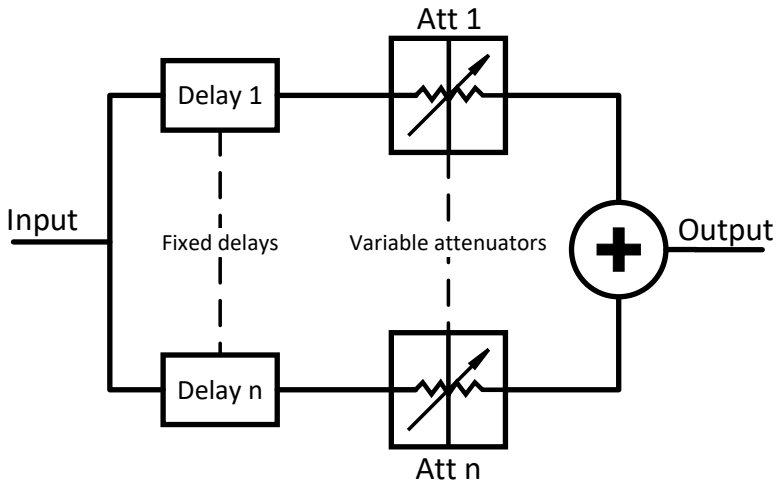

Figure 3.2. *Stanford analog canceller design [27].*

MIT Analog Canceller Design

The MIT research team used a two-tap vector modulator (VM) based canceller architecture where the cancellation signal is first coupled from the transmitter output after a power amplifier (PA), allowing all transmission non-idealities such as harmonics, distortions and intermodulation products to be included and eliminated. The modified cancel output signal is fed back to the receiver input via a low noise amplifier (LNA) used to minimize receiver saturation and non-linearity. [26]

MIT's vector modulator structure is shown in Figure 3.1. First, the signal goes through a 90-degree splitter and then again via a 180-degree splitter. Here, the input signal undergoes a series of fixed phase shifts to produce the four phasors $I+$, $I-$, $Q+$, and $Q-$. These phasors are span out with 90 degree separation. The switches are used to select either the positive or the negative phasor for both the in-phase (I) and quadrature (Q) channels. These phasors are weighted independently using variable attenuators and then merged at the output by a combiner. The phasor selection combined with weighting allows the VM to generate an arbitrary complex response by attenuating and phase shifting the input signal, making it ideal for RF canceller tuning and SI cancellation. [26]

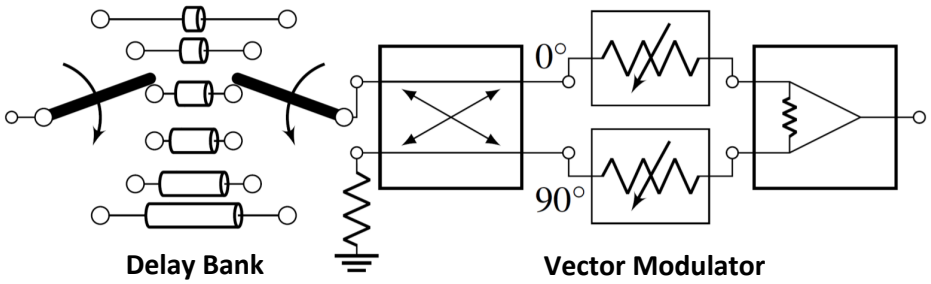

Figure 3.3. *A new proposed RF canceller architecture [30].*

Stanford Analog Canceller Design

The Stanford research team has a quite similar design compared to MIT. Figure 3.2 presents their suggestion for the analog cancellation circuit. The design uses single antenna configuration with a circulator. A small replica of the transmitted signal is attained from the TX chain before it is entering to the circulator. This replica consequently consists of the transmitter non-idealities generated by the TX chain. The replica of the signal goes through a circuit which includes parallel lines of various delays and tunable attenuators. The delays are basically cables with various lengths. The delay lines are then summed, and this signal combination is then subtracted from the signal at the RX path. The circuit design offers copies of the transmitted signal with fixed delays. [27]

3.2 Proposed Cancellation Approach

The new RF canceller design provides full 360-degree vector modulation by introducing an architecture which uses a delay bank in series with a vector modulator. The delay bank provides an initial group delay by choosing a suitable delay line for a certain frequency. The purpose is to delay the phase within 90° of the inverse SI-phase. The vector modulator controls the signal amplitude and provides fine tuning for the phase with 90-degree tuning range.

The RF canceller architecture is illustrated in Figure 3.3, including both the delay bank and the vector modulator designs. The delay bank has two switches which connect the correct line with a fixed delay. The vector modulator then splits the signal into two copies which have 90-degree phase difference between them. Both of these copies are weighted separately by variable attenuators and then combined. In the previous canceller designs, the vector modulator has been implemented by using a single integrated circuit (IC) chip [26, 27], but such a component is not available in the market for high-power applications. Thus, in the proposed canceller design the vector modulator is built using high-power tolerant discrete components.

Delay bank

Designing the delay bank starts by determining the shortest delay length. It can be implemented as a PCB trace or a cable. Other delay lengths are relative to the first one. One delay line with the vector modulator provides 90-degree tuning range. It requires total of four cables to achieve a complete 360-degree phase coverage at a certain point frequency because the delay cables lengths can be selected with 90-degree intervals. The delay bank has to be designed so that the full phase coverage is achieved for the whole frequency band which requires definitely more than four delay cables. A phase map is used for this purpose, in which the coverage area of each delay cable is plotted. The axes of the phase map are frequency and phase. It demonstrates the overlap between the different cables and the union of individual cable coverage areas should cover the whole area. Analyzing the phase map can prove that there appear no gaps at any frequency inside the band.

Phase dispersion at the highest frequency is the limiting factor in the delay design [30]. The delays need to have high overlap between them at the lowest frequency so that there would not be any gaps at the highest frequency. The overlap is increased by adding more delay lines to the design. Total of six delay lines would be enough to cover whole frequency band if the lengths have been tuned so that there is a minimum of few megahertz of overlap between adjacent delays in frequency domain [30]. Overlaps also increase the tolerance for manufacturing errors. For example, the eight delay line design would have better tolerances compared to the six delay line design due to the larger overlaps in the phase map.

In addition, overlaps in the frequency domain contribute towards stable cancellation performance in a changing environment as the conditions around the antenna have direct impact on the SI. For example, if the RF canceller uses a dual antenna configuration where the two antennas swing due to wind which is constantly affecting the phase as the distance between them changes. If the required phase is located right between of two delays on the phase map, where there is only infinitesimal amount of overlap, the canceller would need to constantly swap between these delays while trying to find the optimal cancellation. Cable switching momentarily pauses the cancellation because the switches have some switching delay and the variable attenuators have to be re-tuned. Thus, the overlaps allow the system to stick with one delay even though there are some slight constant changes in the environment.

While designing the delay cables, few factors have to be considered. The total electrical length of the cable is sum of the actual cable and two sub miniature version A (SMA) connectors. A cable can be cut with a certain precision, which introduces always some error. For example, 1 mm error in coaxial cable's length will result a phase error about 0.41 degrees at 225 MHz and 0.73 degrees at 400 MHz. Once the SMA connectors are

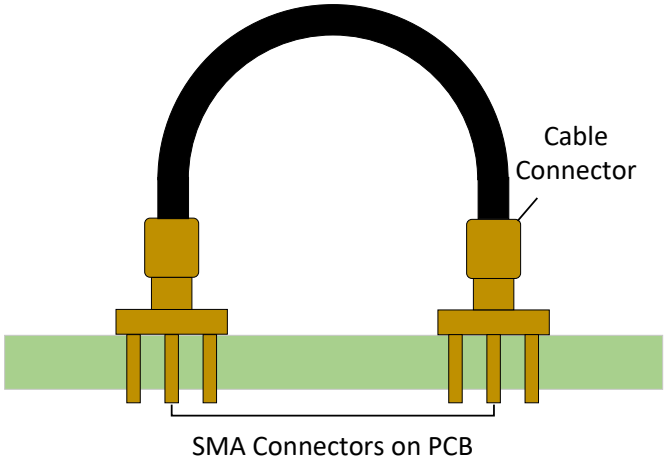

Figure 3.4. *Delay cable connection to the PCB.*

attached to the both ends of the cable, the total length cannot be altered afterwards.

The delay cable is connected between the SMA connectors on the canceller board as shown in Figure 3.4 where the cable will experience some bending. This sets a limitation for minimum length of delay cable. For example, choosing a 100 mm long cable as the first delay cable would be suitable for the practical implementation.

The lengths of the other cables are calculated as additions to the shortest length to yield the correct time delays. A single cable has a phase delay due to its length and in addition an ideal vector modulator provides the adjustable delay from 0 to 90 degrees. This is described by the following equation:

$$\phi_n = \frac{l_n f}{v_p} \cdot 360 + \theta, \tag{3.1}$$

where l_n is the length of the n-th delay cable, f is frequency, v_p is propagation velocity in the cable, and θ is the vector modulator's adjustable delay [30]. The used material for the delay cables is a standard RG-58 coaxial cable with following properties: propagation velocity v_p = 0.66 c_0, attenuation factor α = 0.2 dB/m at 200 MHz, and α = 0.32 dB/m at 400 MHz [31]. Table 3.1 presents the calculated delay lengths for a six-delay line configuration where the first delay $n = 1$ is chosen to be a PCB trace and the others are implemented as coaxial cables.

The phase map for the cable design is shown in Figure 3.5 where each cable coverage is represented by a different color. The cables are in order from top to bottom. The phase is plotted from $0°$ to $360°$. The purpose of the phase map is to demonstrate the overlaps between the delays and to show that no holes are created for any phase-frequency pair. In this case, the hole means a gap in phase coverage. The design has few critical points where holes could appear due to imperfections in the cable manufacturing. [30]

n	l_n [mm]	delay [ns]
1	0	0
2	123	0.622
3	256	1.294
4	377	1.905
5	500	2.527
6	664	3.356

Table 3.1. *Cable design: internal delay and 5 delay cables.*

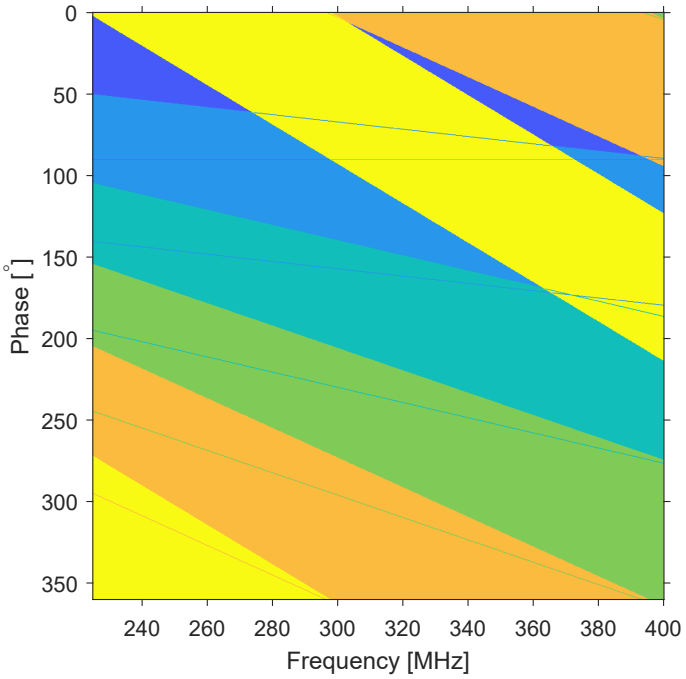

Figure 3.5. *Phase map: phase coverage with six delay lines.*

Delay bank is designed to be flexible and support any delay line configuration from four to eight lines. The first revision the RF canceller prefers delay cables over the PCB trace implementations because trace lengths cannot be altered after the PCB is manufactured. The delay cable design also allows delay optimization for smaller sub-bands inside the design frequency range.

Vector Modulator

The most important function of the RF canceller is to control the phase and amplitude of the coupled RF input signal with 90 degree vector modulation. The canceller's vector modulator must be able to tune input signal's phase and amplitude with high precision for the whole frequency band. The phase has to be exactly opposite to the received self-interference and the amplitudes must be equal [30]. The vector modulator structure is shown in Figure 3.3 where the input power is first divided into two components by the

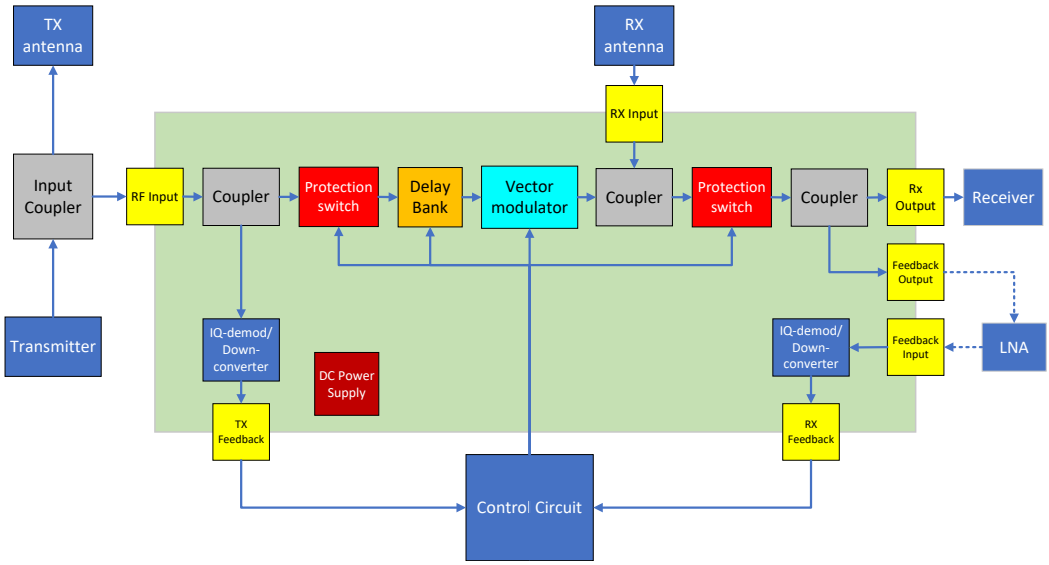

Figure 3.6. *Block diagram of the proposed self-interference. cancellation circuit*

90-degree hybrid.

These components are referred as in-phase (I) and quadrature (Q) which are both scaled by an individual variable attenuator and then merged by a power combiner. This yields the cancellation signal that is combined with the received SI signal. The phase tuning is achieved by weighting the I- and Q-components. The range is from 0 to 90 degrees where minimum and maximum ratings are reached where either the I- or Q-component is fully suppressed. If the 90-degree hybrid's input signal is in form of $\cos(wt + \phi)$, mathematically these I- and Q-components can be expressed by the following equations:

$$\begin{aligned} I &= w_I \cdot \cos(wt + \phi) \\ Q &= w_Q \cdot \sin(wt + \phi), \end{aligned} \tag{3.2}$$

where w_i and w_q are the weight values and ϕ is the initial delay provided by the delay bank. By selecting the initial delay and weighting the I and Q components separately, a complex response is created by combining these components. This should correspond to the received SI on a complex plane for a successful cancellation.

The proposed design for the variable attenuator is to utilize PIN-diode based attenuators which have a wide operation frequency range from 10 MHz to 5 GHz [32, 33]. The key benefits for the RF canceller design are constant impedance over broad bandwidth, wide dynamic tuning range and reasonable high power tolerance. The attenuation is controlled by a DC voltage. The PIN-diode attenuator circuit's operation is explained later in more detail in Section 4.2.3.

RF Canceller Board

The delay bank and the vector modulator do not create a fully functional RF canceller by themselves as they need some additional components around them to complete the circuit. A high-level block diagram of the proposed RF canceller design is shown in Figure 3.6. The green rectangle represents the actual RF canceller board, while the other items outside are external devices or components when the canceller is used as part of a larger system. There are three couplers, two protection switches, two delay switches, 90° hybrid, two PIN-diode attenuators, a power combiner and two I/Q demodulators. The design has two main RF signal lines, one is from to RF input to RX output and the another one is from RX input to RX output. These paths are combined at the second coupler on the board as it combines the modified sample signal with the SI signal from the RX antenna. This is the place where the actual SI cancellation happens. Yellow boxes denote input, output and feedback connections.

In terms of cancellation, it is desired to have almost equal power levels for cancellation and SI signal, where the cancellation signal would be a few decibels higher with the minimum attenuation. This ratio can be adjusted by selecting a suitable input coupler relative to the available antenna isolation. There should also be a minimum amount of losses in the RX path as these do not count as cancellation because both signals are attenuated equal amount. Thus, absolute mandatory components are only placed on the RX path with minimal losses as possible. The two most critical pieces are the protection switch and the feedback coupler.

The input coupler is chosen to be an external component, which makes it easy to replace and allows transmission power scaling. It provides a sample of the TX signal for the RF canceller board as the coupled port is connected to RF input. By changing the input coupler value, the ratio between TX power and RF input power can be adjusted, while keeping the RF input power constant. This feature will be useful during the measurements, because the used TX power can be reduced without affecting the RF input power. For example, when using 100 W TX power and the 20 dB input coupler, 1 W of power will be entering the canceller board.

Couplers are preferred over power splitters because they introduce only small amount of main RF line losses and provide low power samples of the signals for the feedback due to their coupling ratio. The canceller design has total of three couplers on board. The first and the third couplers provide the samples of TX input and RX output as feedback signals which are then down-converted by the I/Q demodulators so the control board would be able to process them more easier.

The protection switches have two purposes. First, they can be used to stop the cancellation without having to turn off the transmitter which is beneficial for applications such as

jamming. Without any cancellation, the RX signal power might be too high for the receiver so it would be useful to have an ability to disconnect the RX antenna from the receiver. Secondly, the input switch can be used to protect more sensitive delay bank switches while selecting correct delay line with high input power. Also, the delay switching may cause transients that might be harmful for the receiver or may affect the control circuit performance.

The RF canceller board has a DC power supply to provide operating and biasing voltages. Different IC components will likely need slightly different operating voltages that can be implemented with either one or a pair of rail voltages. By using the voltage division, the bias voltages can be adjusted and each voltage does not require its own rail. The power supply also includes the input terminals for the voltages and a ground connection. The input voltages are regulated and filtered. It also has an indicator to see if the power is on or off.

The feedback signal from the RX output has an option be amplified by an LNA if the signal power is considerably low. An LNA is designed as a special type of amplifier that adds only small amount of noise to the input signal. A weak feedback signal needs amplification, otherwise it will be lost in the quantization noise if the ADCs on the control board have very limited amount of bits available. If the input signal has already high power, the LNA is saturated and the output is heavily distorted. Thus, the LNA is not needed in this case. The LNA is optional as the RF canceller board is designed prior to the control circuit and its specifications are yet unknown. If the LNA option is left unused, the feedback output is directly connected to the feedback input with an external coaxial cable.

3.3 Impairments

When it comes to analog signal processing and theory, there are always certain impairments that have to be taken into account in order to improve overall performance of the device. The most common impairments for the RF canceller are noise and distortion caused by non-linearity which are discussed in this section.

Noise Figure

Noise represents an interfering and unwanted power in an electrical system. The total noise measured for a certain bandwidth at the input or output of a device is the integral of the spectral noise density over the bandwidth when the signal is not present [34, 35]. All of the components add their noise to the signal. This signal-to-noise ratio (SNR) degradation of is known as the noise figure (NF). The noise figure can be determined for all kinds of components such as cables, attenuators, amplifiers, etc. For passive devices, the NF is equal to their insertion loss also known as a S21 parameter [35]. The NF can be

improved by placing the noisiest component last in cascaded systems, because NF of the first device affects the most to the overall system's NF according to the Friis equation [34]. The RF canceller design prefers components with a small NF as the noise generated by the components cannot be cancelled and decrease the performance. The noise power P_N generated by a component is calculated as

$$P_N = kT\Delta f, \tag{3.3}$$

where k is the Boltzmann's constant, T is temperature in kelvins and Δf is the bandwidth. [34] The minimum noise level that is measured in an electronic system is the thermal noise floor similar to the white noise. It can be calculated as power per bandwidth so it results in about -174 dBm/Hz spectral power density in room temperature [36]. Usually estimating and analyzing the noise is difficult as there are a variety of intrinsic noise sources which are unique to specific systems. The minimum noise floor is set by the thermal noise while all other noise sources are absent. The thermal noise floor can be only reduced further by decreasing the operation temperature for the components. It is not practical to operate under the room temperature as component performance is affected when approaching their minimum operation temperatures.

A spectrum analyzer is used to measure the noise floor. Any noise source that is more intense will be seen above the thermal noise floor. This will help to identify unexpected noise sources during the cancellation measurements. The receiver and the measurement device's have also their own noise floor that sets a hard limit for the cancellation.

Non-linearity

The RF canceller design has components such as switches that contain transistors and PIN-diodes that can cause distortions. The 1 dB compression point (P1dB) is defined as the power level at which the output power of a device no longer follows the linear input-output power curve and reaches a point where the actual response is 1 dB lower than the theoretical response [37]. This input-output curve is also known as a small signal gain [35]. Once a device reaches its P1dB, it transitions from a linear region to a compression region and the actual response becomes a non-linear. The device starts producing distortion such as harmonics, and intermodulation products [37]. These distortions can further combine and start generating spurious signal components. As shown in Figure 3.7, when the input power level increases, there comes a point where the output power no longer increases by the gain value, the device's output power starts to saturate until it reaches the saturation power P_{sat}. IP1dB and OP1dB refer to the input and output values of the 1 dB compression point.

PIN-diode attenuator's P1dB compression point changes with respect to control voltage and it is not constant for different operation frequencies. Usually, low control voltages

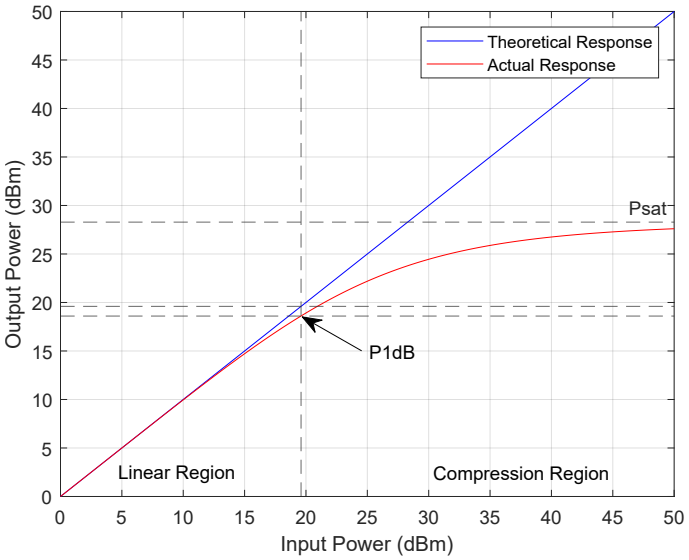

Figure 3.7. *P1dB compression point and operation regions.*

from 0 V to 1 V weaken significantly the P1dB power level [32, 33] and that may restrict the usable operation voltage range. From the RF canceller perspective, the PIN-diode attenuators cannot provide their maximum amount of attenuation as the highest values are reached with lowest control voltages.

The RF input signal can contain multiple frequency components such as carriers, which make it vulnerable to intermodulation distortion (IMD). It occurs when two or more signals enter a non-linear system [37]. If the RF spectrum is measured at the output of the non-linear device, the results will show original input signals together with the sum and difference of the input signals and also including their harmonics. So, if a non-linear system has two input signals, for example at two different frequencies f_1 and f_2, now the non-linearity creates second-order intermodulation signal components. These new frequency components are $f_1 + f_2$, $f_2 - f_1$, $2f_1$ and $2f_2$ [37]. The terms such as $2f_1$ and $2f_2$ are multiples of the frequency which are known as harmonics. All of these frequencies are considered undesirable. [34]

These second-order intermodulation products are then mixed with the original signals, creating third-order intermodulation products [37]. These products have normally very low power and are hidden under the noise floor when the RF canceller or any other device is operating in the linear region [38]. But increasing the RF input power will shift the operation towards the non-linear compression region. The intermodulation products emerge above the noise floor and start causing issues. The third order intermodulation products are created by the original signals and the second-order intermodulation products, when they are added or subtracted to form every possible signal combination [37]. However, these intermodulation products are typically far from the original signal and therefore can easily be filtered. There are only two problematic intermodulation products, which are $2f_1 - f_2$ and $2f_2 - f_1$. These frequencies are the main source for the IMD as

it is hard to filter them out without affecting the original signal since they are close in the frequency domain [37]. The intermodulation distortion value is typically measured using the intersections of the linear response and the third intermodulation response. Similar to 1 dB compression point, it can be defined for either input or output powers. [34]

In order to avoid aforementioned distortions, the RF canceller should be operated with a reasonable input power that will not force the components into compression region. This is so called back-off operation where the device operation point is far enough from the P1dB compression point. The effects of non-linearity are seen as the total cancellation decreases when the input power increases.

4. RF CANCELLER DESIGN AND IMPLEMENTATION

In this chapter, the PCB design process of the RF canceller board with the proposed architecture is presented. Starting from component choices, describing the PCB stack-up structure, explaining dielectric material choices, showing component placements and providing some insight to both electromagnetic compatibility (EMC) and power management. The schematics and layouts are drawn by with KiCAD which is a free-to-use cross platform and open source electronics design automation suite.

4.1 Overview

A component level block diagram is shown in Figure 4.1. This diagram has more detailed PCB structure than the initial design plan presented in Figure 3.6. The previous functional blocks are now divided into specific component types but the color-coding is the same. Couplers are presented as gray, protection switches are red, delay bank parts are orange, vector modulator's components are light blue and I/Q-demodulators are blue. The specific component choices are explained in Section 4.2. All of the RF signals are connected to the board via SMA connectors which are presented with yellow boxes at the edges. Thus, control circuit and external components, such as an input coupler, antennas and amplifiers can be easily connected to the board.

The delay bank has only one fixed delay implemented as internal PCB trace which allow testing without need for the delay cables. Other delays are implemented as coaxial cables. Each delay cable needs two SMA connectors on the PCB. When all of the input, output and cable connectors are added together, the RF canceller board has total of 27 SMA connectors so there must be some physical space around each one that they can be opened and tightened with an SMA torque wrench. So they have to be span around which will increase the total size of the board.

The PCB must be rigid because the delay cables place extra weight on the board when they are attached. The canceller board must be supported at multiple points, otherwise it may bend in the middle if the supports are only located in the corners. The dielectric materials and the PCB stack up is specified in Section 4.3.

Figure 4.1 does not show the connections for control or operation voltages. The DC power

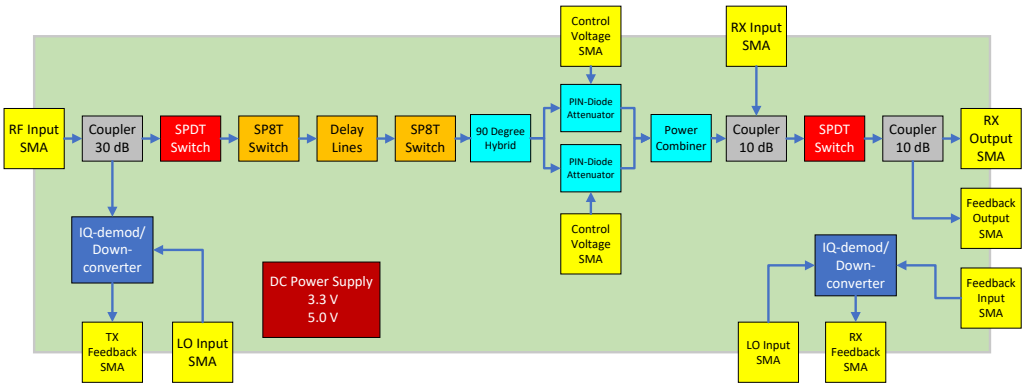

Figure 4.1. *Component level block diagram of RF canceller board.*

supply design is presented in Section 4.3.2. Logic level control signals for the delay bank and the protection switches are connected by a flat cable or a twisted pair. The required control signals are explained more thoroughly in Section 4.3.5.

4.2 Components

In this section, the key components of the RF canceller are presented and why they were chosen for the first revision of the board. The design has a total of 178 component pieces, using both through hole technology mounting (THT) and surface mount technology (SMT). SMT components are also known as surface mount devices (SMD) which are more efficient, cost effective and adapted to denser PCBs [39]. SMD components are generally preferred in this RF canceller prototype. However, THT components still provide great attachment strength which is useful in case of on-board connectors. Only the selection criteria for the most important RF and IC components are discussed in this section. These components are chosen by the following principles:

- The operation frequency must at least cover the entire bandwidth from 225 MHz to 400 MHz. Most of the components work over a wide bandwidth, but it is preferred to check that the operation does not change significantly at lower frequencies.
- Power tolerance defines the maximum RF input power but also denotes the maximum power dissipation in the component. The power dissipation is equal to the insertion loss so it is desired to have minimal losses.
- Components should have $50\ \Omega$ input and output impedance which allows different parts to be connected without any extra impedance matching circuitry. In addition, it reduces frequency selectivity issues.
- The DC power supply for the ICs is preferably single-sided and as many components as possible should use the same operating voltage. Having a negative rail would complicate the design by affecting the signal routing.

- Especially the ICs should require small amount of external components and have minimum number of control signals. This will later facilitate device testing and control circuit design.
- All components must be available at consumer suppliers, i.e., Digikey, Farnell or Mini-Circuits. The RF canceller board is to be built without any custom parts or components.

The following subsections are divided so that each of them cover a component selection for one functional part of the RF canceller. For each component, the most important requirements are presented and the most suitable component is chosen based on them. ADS simulations are used to support a certain component decision.

4.2.1 Protection Switches

The RF canceller is performing a hot-switching operation while a control circuit changes the delay lines in order to find optimal initial delay value. Hot-switching is defined as a transient condition where a switch or relay is either opened or closed while RF power is present at the terminal [40, 41]. Hot-switching has a major impact on switch or relay life time because the switch will experience contact erosion and heating. The contact erosion is sufficient to weaken the RF performance [40]. Same conditions does not occur in a cold-switching where the RF signal is removed before changing the state [40].

In RF hot-switching, a problem can occur if the source voltage standing wave ratio (VSWR) is high. Reflected waves may build up a high voltage which appears across an open contact. Insertion losses in the RF path will slightly reduce the maximum voltage due to the attenuation of the reflected signals. High voltages cause arcing shortly before the switch is fully closed or opened [40]. When hot-switching AC or RF signals, the arc will often be extinguished, because voltage is not constant and passes through zero twice per cycle [41]. Also, operating the switch with high frequency will not only cause arcing, but increase the temperature inside the component [40]. So extra cooling elements may be needed to reduce the operating temperature.

Most of the SMD switches have low hot-switching capability or it is not specified. Component vendors may provide some information on ratings, but they have to provide these ratings under reproducible conditions which usually means they are specified with resistive sources and loads [41]. Finding a reliable single-pole six-throw (SP6T) or single-pole eight-throw (SP8T) switch for the delay bank would require some extra testing and experimenting with different switches. So it is decided that a single-pole dual-throw (SPDT) switch is placed before the delay switches to provide the hot-switching capability and protect the more sensitive components in the board.

The chosen protection switch is TS7225FK from company Tagore Technology which

would be at the input to disconnect the TX chain. A second TS7225FK is placed in the receiver path to disconnect the RX chain even though it is unlikely that the hot-switching capability is needed there, since the power in the RX input will be significantly lower than the TX power. However, it can be used to protect the sensitive receiver from strong transients that may occur during switching.

TS7225FK is a symmetrical reflective SPDT switch designed for hot-switching applications. It operates on a broadband from 10 MHz to 6 GHz frequencies. The TS7225FK is an excellent choice for this application especially due to its 40 dBm hot-switching capability. Also it has high isolation and high linearity within a small plastic quad-flat no-leads (QFN) package. It operates within versatile range of power supply values 2.6–5.5 V. In addition, the datasheet suggests that higher supply voltage increases the hot-switching performance, so it would be optimal to apply maximum supply voltage. [42]

4.2.2 Delay bank

If the canceller only operates at a certain frequency point and any margin is not needed, then four wires are sufficient because cable delays can be selected at 90-degree intervals. However, for the wide frequency band (225–400 MHz), the phase dispersion of the different cables make it impossible to cover all possible phases on each frequency without gaps on the phase map with four cables. For the wide frequency band, it is determined that at least six delay lines would be needed [30]. However, the safest solution would be eight delay lines for better coverage because the phases have greater overlapping area and they reduce the risk of having gaps in the phase map due to manufacturing errors. In practice, this means, that some of the cables are either slightly shorter or longer than their designed lengths. In addition, operation can be avoided at the edges of the tuning range where the canceller is especially prone to non-linearity.

Delay bank requires at least an SP6T type of RF switch but we prefer an SP8T switch for more flexible cable designs. The delay bank is already protected by an SPDT switch as mentioned in the previous subsection. Thus, hot-switching capability is not needed, but it should have decent RF input power value to maintain its operation while high-power continuous wave (CW) is applied. By choosing the SP8T switch, any number of delay lines can be constructed up to eight in total. The canceller board has one fixed internal delay line implemented as a PCB trace with a length of 50 mm. The other seven delay lines are done with coaxial cables. It is not a mandatory to use the internal delay, but it allows some degree of testing, if the delay cables are missing or yet to be manufactured.

The chosen SP8T switch is SKY13418-485LF from company Skyworks Solutions designed for frequencies from 100 MHz to 3.8 GHz. It provides high linearity and insertion loss is 0.45 dB at the 225–400 MHz band. Maximum RF input power is 37.5 dBm. It has a versatile power supply range from 2.5–5.0 V, while 3.3 V is recommended. [43]

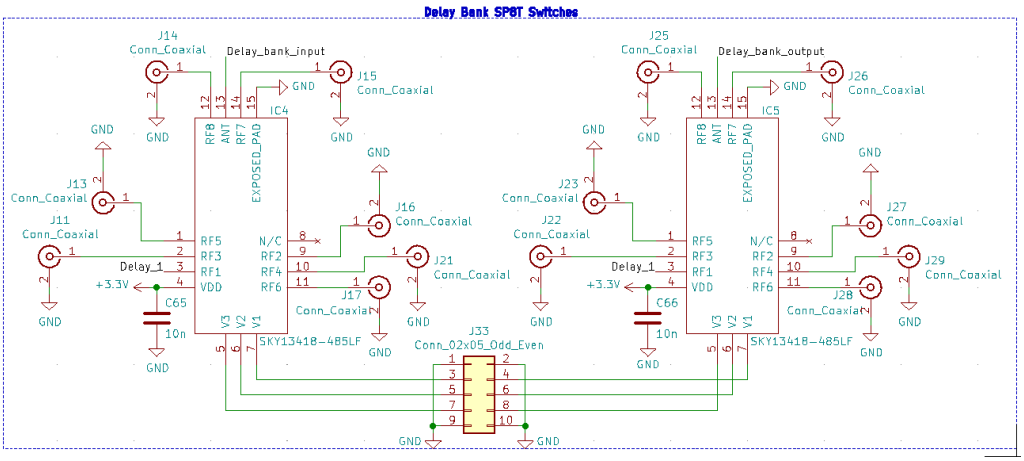

Figure 4.2. *Delay bank schematic.*

	Designed		Measured		
n	**l_n [mm]**	**delay [ns]**	**delay [ns]**	**min loss [dB]**	**max loss [dB]**
1	100	0.505	0.518	0.05	0.07
2	225	1.137	1.124	0.11	0.14
3	357	1.804	1.799	0.12	0.15
4	479	2.421	2.392	0.13	0.17
5	601	3.037	3.019	0.16	0.21
6	760	3.841	3.816	0.19	0.25

Table 4.1. *Old cable design and measurements [30].*

Figure 4.2 shows the KiCAD schematic for the delay bank. Each RF path has vertical SMA connectors for delay cable connections, excluding the internal PCB trace. Control signals for both switches are connected via a 2x05 male pin-header.

The cable design is shown in Table 4.1 which were originally manufactured as a part of the proposed vector modulator concept for the article [30]. By comparing the designed and measured delays, there are some variation in the cable lengths due to manufacturing inaccuracy. Approximately, the error is from 1 mm to 3 mm per cable. These cables are later used for the measurements because there is no critical need for the new improved cable design that is calculated in Table 3.1.

4.2.3 Vector modulator

The most important part of the RF canceller circuit is the vector modulator which is implemented with discrete components including: a 90° hybrid, two PIN-diode variable attenuators and a power combiner. All of them are high-power tolerant components. During active operation, the components must sustain a stable performance with high linearity even if several watts of power goes through them.

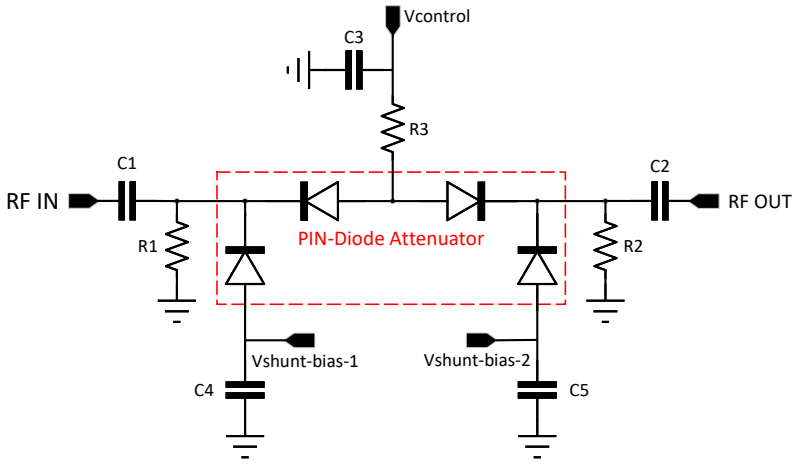

Figure 4.3. *PIN diode attenuator circuit.*

First, the QCN-3+ from Mini-Circuits was chosen as the $90°$ hybrid, but it is also known as power splitter or combiner. It has operating frequency range from 220 MHz to 470 MHz which perfectly covers the designed frequency range. It has about 0.4 dB insertion losses and maximum power rating is 15 W when used as a splitter. The amplitude imbalance is between 0.05–0.77 dB. Phase imbalance increases towards higher frequencies, starting from $0.40°$ and reaching about $4.0°$ at 400 MHz. [44]

The variable PIN-diode attenuator circuit is shown in Figure 4.3 and it was also built as a separate PCB for evaluating and testing purposes. The circuit is also known as a quad PIN Diode π-attenuator. The four PIN diodes are obtained as an integrated SOT-25 or similar package whereas the other components are discrete. The PIN diodes are utilized as a Waugh-attenuator [32]. The component has five terminals: RF_{in}, RF_{out}, $V_{control}$, $V_{shunt-bias-1}$ and $V_{shunt-bias-2}$. The attenuation is DC controlled by $V_{control}$, ranging from 0 V to 20 V, which will result in about maximum 40–45 dB of attenuation [45].

In the circuit, capacitors C1 and C2 are DC blocks and prevent both bias voltages and currents leaking. R3 acts as a current limiter. Capacitors C3–C5 provide stable control and bias voltages. Resistors R1 and R2 serve as bias returns for the series diodes in the main RF line [32]. The attenuator is tuned by changing these two resistors together with shunt-bias voltages. If the values are properly selected, they will correctly balance the bias current between the series and shunt diodes. Good impedance matching has to be maintained over entire dynamic range of attenuation [32]. The optimal resistor values can be obtained via simulation, but it requires accurate models for the PIN diodes. Thus, simulations may provide a decent initial value for resistance, but this should be verified with empirical testing [32].

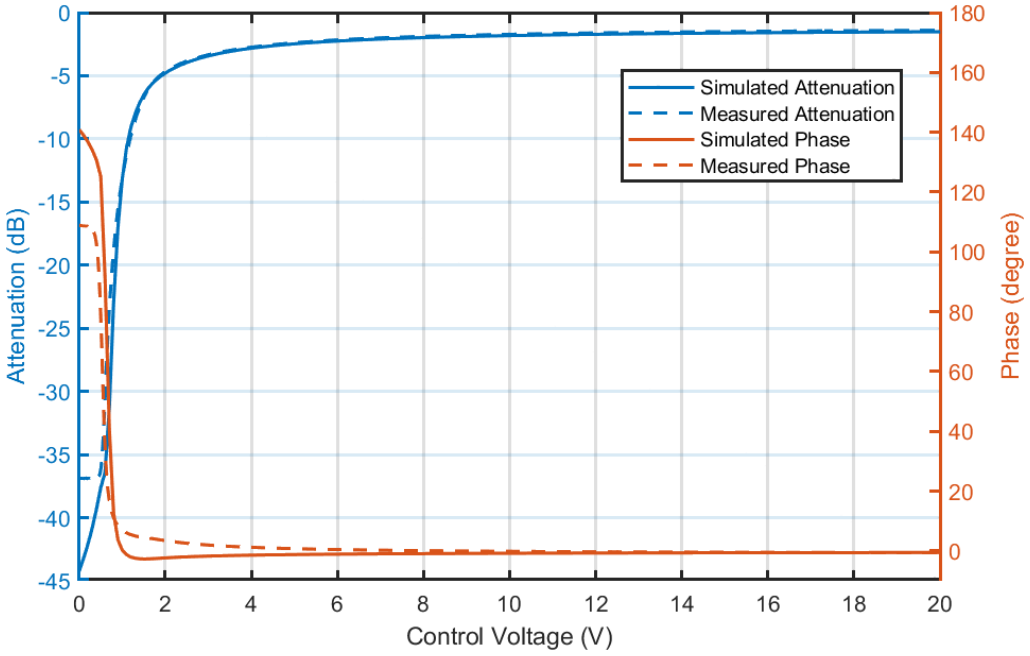

Figure 4.4. *PIN-diode simulation and measurement results.*

When a PIN-diode is operated above its cut-off frequency, it behaves like a voltage controlled variable resistor. The cut-off frequency is defined by the carrier-life-time and it can be calculated with the following equation:

$$f_c \geq \frac{10}{\tau}, \tag{4.1}$$

where τ is the carrier-life-time. PIN diodes should not be operated near the cut-off frequency because it predisposes the diode to non-linear intermodulation and harmonic effects. This is caused by the modulation of the charge carrier concentration. [46] For example, if $\tau = 1.25\ \mu\text{s}$, it will result 8 MHz of cut-off frequency. However, the τ is not constant as it decreases when the input power increases. Thus, the cut-off frequency gets shifted towards higher frequencies. [46]

While choosing the PIN-diode, several pieces from different manufacturers were simulated, purchased and tested. The PIN-diode's simulation model is confirmed by comparing simulation results against measurements as shown in Figure 4.4. The parameters of interest are attenuation and phase as a function of control voltage. The measured values correspond to the simulated values except at the lowest control voltages where there are some difference in both attenuation and phase. These type of simulations were run over the entire frequency band for each PIN-diode.

Finally, BAP70Q-125 was chosen from NXP Semiconductors mainly because its attenuation curve was slightly more gradual with low control voltages, even though there were other potential candidates. The RF canceller would probably have worked fine with any of the tested PIN diodes as all of them behaved similar to each other.

The last component of the vector modulator is the power combiner, which utilizes a Wilkinson power divider structure [47]. It combines the I and Q branches. Its power dissipation depends on the relative signal amplitudes. [30] SYPS-2-52HP+ from Mini-Circuits was chosen as power combiner because it has low insertion loss, typically 0.5 dB, maximum internal power dissipation is 6 watts and maximum RF input power of 15 watts [48].

4.2.4 Directional Couplers

The RF canceller design utilizes few directional couplers on the board. Couplers are passive devices used for signal processing. They sample the input signal with a predetermined degree of coupling, creating two output signals [49]. These two output signals have unequal amplitudes. The larger signal passes through the main RF line which is typically between ports 1 and 2. [49] The smaller sampled signal is delivered to the coupled port which is port 3. Coupling factor is the ratio between input power and the power at the coupled port. Directivity describes the coupler's ability to separate propagating waves in forward and reverse directions. Isolation shows the amount of power that is delivered to the uncoupled port which is typically labeled as port 4. Insertion loss indicates signal attenuation in the main RF line, the theoretical minimum for the insertion loss depends on the coupling factor [49].

Directional couplers are either 3- or 4-port networks. The 3-port coupler has internal termination that is specific to a component type and it is non-removable. The four-port couplers are also known as bi-directional. These type of couplers operate in the reverse direction when the input signals are connected to ports 2 and 3 and the combined output signal is seen at port 1. Port 4 would be the coupled port in this case. Bi-directional couplers perform equally well in both forward and reverse configurations. [49, 50]

The first coupler on the board needs to have high power tolerance and low insertion losses. Also, the coupling factor should be reasonably high, since it couples a sample of the signal that enters the RF input. This sample is for the control circuit and cannot have a high amplitude so the required coupling is from 20 dB to 30 dB. The second coupler is operated in the reverse mode as it combines the cancellation signal with the RX input signal. The coupler does not require high coupling value but should have low insertion loss so it does not cause unnecessary amount of attenuation for the received signal. So choosing either a 6 dB or a 10 dB coupler should be sufficient. The third coupler provides a sample of the RX output signal to the feedback. This coupler also requires a low insertion loss as the received signal passes through it before entering the receiver. Its coupling value should chosen so that both samples would preferably have similar power levels as they enter the control board.

Based on previous specifications, three bi-directional couplers were chosen from the Mini-Circuits catalog. The input has a MBDA-30-451HP 30 dB coupler with an excellent power

handling capability up to 200 W and low main-line insertion loss of 0.15 dB [51]. The another two couplers for the RX input and the feedback are SYBDC-10-13HP+ with 10 dB of coupling and 0.95 dB of insertion losses. They also have a decent power handling capability, up to 10 W [52]. RX chain has overall lower power handling requirements than the TX input.

4.2.5 I/Q Demodulator

Two I/Q demodulators are needed to down-convert both samples of input and feedback signals from RF to baseband (BB). By using the down-conversion, signals are frequency shifted to BB which is centered around DC. The input I/Q demodulator requires both a local oscillator (LO) signal and the actual RF signal. The output baseband signals are split to I and Q components. Now, the control signals are processed in BB which is better than processing them in RF, because the sample rate of the ADC can be much lower.

The local oscillator signal is to some extend leaking into the output, which means that it has to be filtered out. This is done by adding low-pass baseband filters for both I and Q outputs. For example, a high-order Butterworth filter could be suitable for this purpose with a cut-off frequency from 10 MHz to 20 MHz. The high-order filter design provides better roll-off rate resulting in a narrower transition band at the cost of a more complex design and an increased number of passive components. [53]

The I/Q demodulator should be able operate at the low frequencies 225–400 MHz with a reasonably low noise figure (NF). High linearity is also required which guarantees that the demodulator will not saturate even if the cancellation is working poorly. The another requirement for I/Q demodulator is to have minimum amount of control signals and external components as some I/Q-demodulators may need additional control voltages to set up different bias voltages. Overall, it is not ideal for practical testing either. Also, the needed power supply has to be single-sided and in reasonable range for the RF canceller board. Something between 3.3–5.0 V would be optimal.

The ADL5387 from Analog Devices was chosen with RF operating frequency range from 30 MHz to 2 GHz, which covers the designed bandwidth. ADL5387 has a NF of 12.5 dB at 300 MHz, IP1dB = 12.7 dBm, and IIP3 = 32 dBm at 300 MHz. The differential RF inputs provide a broadband input impedance of $50\ \Omega$ and are driven with a 1:1 balun that transforms a balanced transmission line to an unbalanced for optimal performance [54, 55]. The required LO frequency is two times the RF input frequency. Thus, the down-converted frequency is calculated using the following equation:

$$f_{Down-Convert} = \frac{1}{2} f_{LO} - f_{RF}. \tag{4.2}$$

According to previous equation and ADL5387's datasheet, a sixth-order low-pass Butter-

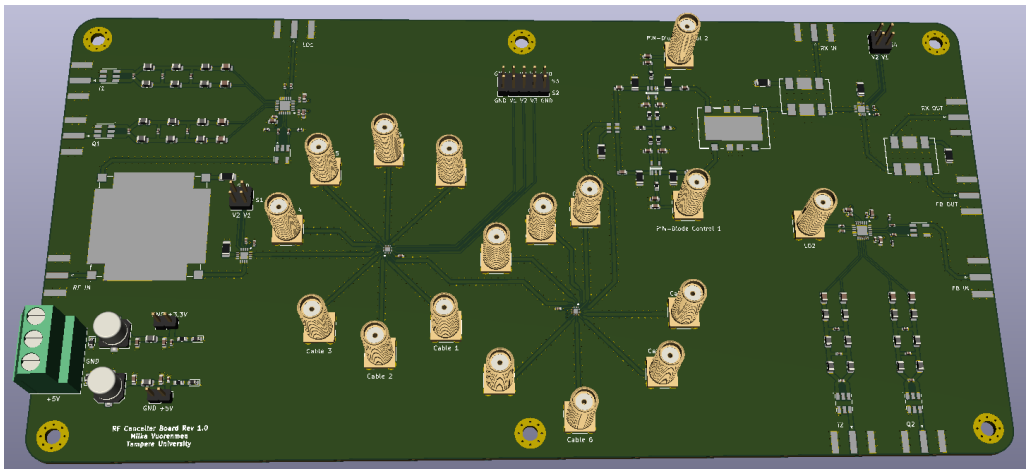

Figure 4.5. *RF canceller's KiCAD 3D model.*

worth baseband filter is recommended with cut-off frequency of 10 MHz. It prevents the LO from leaking into I and Q outputs. The filter is designed and simulated with ADS. The simulated filter response is shown in Figure 5.7.

4.3 PCB Design

This section describes the PCB layer stack-up, the RF trace impedance matching, power supply design, electromagnetic compatibility (EMC) and provides some insight into power and thermal management. Also, outlines for the control circuit interface are defined. The RF canceller's 3D model from KiCAD is shown in Figure 4.5. The model is only missing the horizontal SMA connectors and 3D structures for the couplers and power combiner.

Planning of the multilayer PCB stackup is important because it has a direct impact on the device's performance as it improves signal integrity, reduces electromagnetic emissions and simplifies signal routing. The RF canceller board requires the multilayer PCB stackup because usage of two sided board would significantly restrict the PCB design. The necessary amount of layers would be four, where the top layer is used to route the RF signals. Below the RF layer is a ground plane to minimize loop area and reduce the inductance of the return path [36]. The third layer is a dedicated power plane which is mostly used to route control, biasing and operating voltages to the ICs. The fourth layer is the bottom side and it is yet an another ground plane used mainly for thermal management. The layer stack up is presented figure 4.6, including the height of the each layer, material type and electrical properties.

The chosen material is Rogers 4350B with ϵ_r of 3.66 which is common for RF applications. The Rogers 4350B is quite fragile on its own and bends easily so the inner core has to be rigid. This core material is usually called prepreg which is a cured fiberglass epoxy resin with copper layers attached to both sides. Here, the core consists of two different materials PR7628 and PR2116.

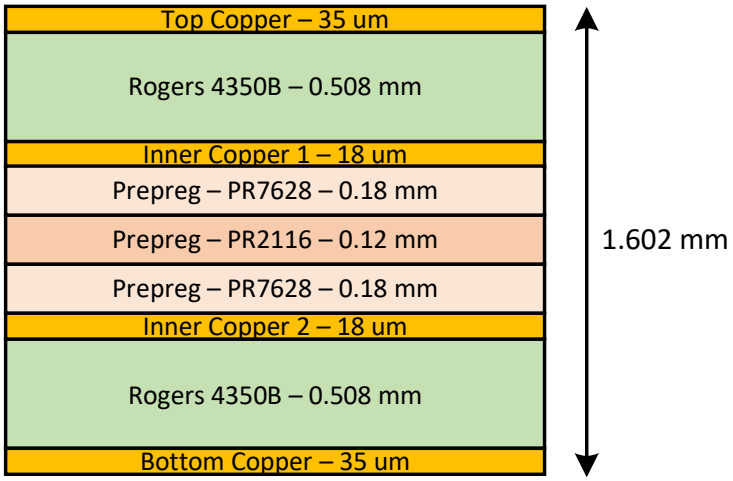

Figure 4.6. *PCB stackup structure and materials.*

The PCBs are ordered from the company Eurocircuits with an assembly service, in order to receive a high-quality product even though the total price is higher compared to self-made boards. External manufacturer is preferable as some of the ICs requires high precision placement and re-flow soldering. The PCB may also have high number of small vias for the RF traces and thermal management. Overall, automized manufacturing will minimize the manufacturing errors during the process. Most likely some of the biasing resistors and decoupling capacitors values may need to be tuned when the finalized product is received. This has been taken into account by picking a reasonable package size (0603 or 1206) for the components and adding larger pads for hand soldering.

4.3.1 RF Traces

PCB trace technologies, such as microstrip and grounded coplanar waveguide (GCPW), also referred as coplanar here, have both their strengths and weaknesses, but these two need to be analyzed and compared against each other to see how they perform, and to make a decision on which one to use on the RF canceller board.

Microstrip structure has a thin transmission line (TL) on one side of a dielectric substrate and a large metal ground plane on the other side. The performance of a microstrip transmission line is affected by variables based on material properties and geometry, including the dielectric constant, dielectric material thickness, TL thickness, and the roughness at the copper-substrate interface. [35] These variables are often presented in the TL simulation softwares, such as ADS or KiCAD.

Coplanar structure increases the ground area in a circuit compared to microstrip by adding two extra ground planes on the both sides of the transmission line, while still having a large ground plane on the bottom layer. The electrical stability is achieved by surrounding the signal line with ground planes as it decreases the coupling through air

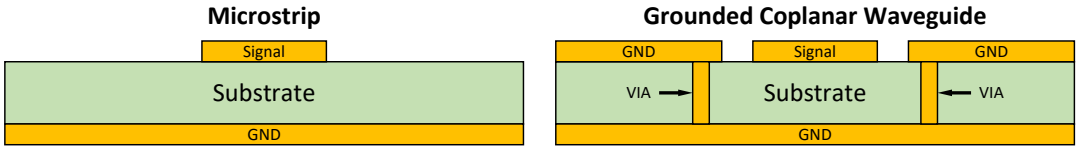

Figure 4.7. *Microstrip and GCPW trace structures.*

domain [56]. Coplanar PCBs are mechanically more complex to fabricate due to the small via size, placement and dense spacing. [35] The both PCB trace structures are shown in Figure 4.7.

On one hand, coplanar circuits have wider effective bandwidths than microstrip circuits. On the other hand, microstrip circuits are easier to manufacture without using industrial PCB process technologies. In addition, the overall microstrip structure is robust due to the fact having a ground plane only on the bottom layer. Coplanar circuits have a better high frequency performance compared to microstrip circuits if the PCB is properly manufactured. Especially, they excel at frequencies in the millimeter-wave range because they have lower dispersion and radiation losses compared to microstrip lines [35, 56].

For example, a small increase in conductor thickness will cause stronger EM-fields appear between the signal and ground planes in the coplanar structure. Also, it creates taller conductor walls, while causing a more of EM-propagation in the air around the copper conductors. Both effects are decreasing the effective dielectric constant of the board. For microstrip board, the effect in effective dielectric constant significantly weaker, if the same increment in conductor thickness is assumed. [56] In both cases, increasing the conductor thickness will decrease the insertion losses [35].

It has been shown that microstrip's performance is not greatly affected by circuit fabrication errors while coplanar has higher sensitivity on errors. Normal variation in the etching process always causes small inconsistencies in conductor spacing and conductor thickness but microstrip structure will provide consistent measurement results [56]. So it is suitable for prototyping and evaluation before ordering the final product.

When the EM-field distributions are analyzed at vicinity of the both TL structures, a wave pattern familiar to quasi-transverse-electromagnetic (quasi-TEM) propagation mode can be noted [35, 56]. In a coplanar circuit, EM-field energy mostly propagates through the air domain around the PCB, because air has a lower dielectric constant than a conductive metal or dielectric material [56]. Thus, wider conductors are used in order to reduce insertion losses in the TLs. [35]

The coplanar technology was selected for use in TLs because it maximizes the ground plane area at the top layer which has all of the SMD component placements. The potential problems with fabrication and vias can be mostly ignored because the PCB is ordered from an external manufacturer which is capable of printing the TLs with a high precision.

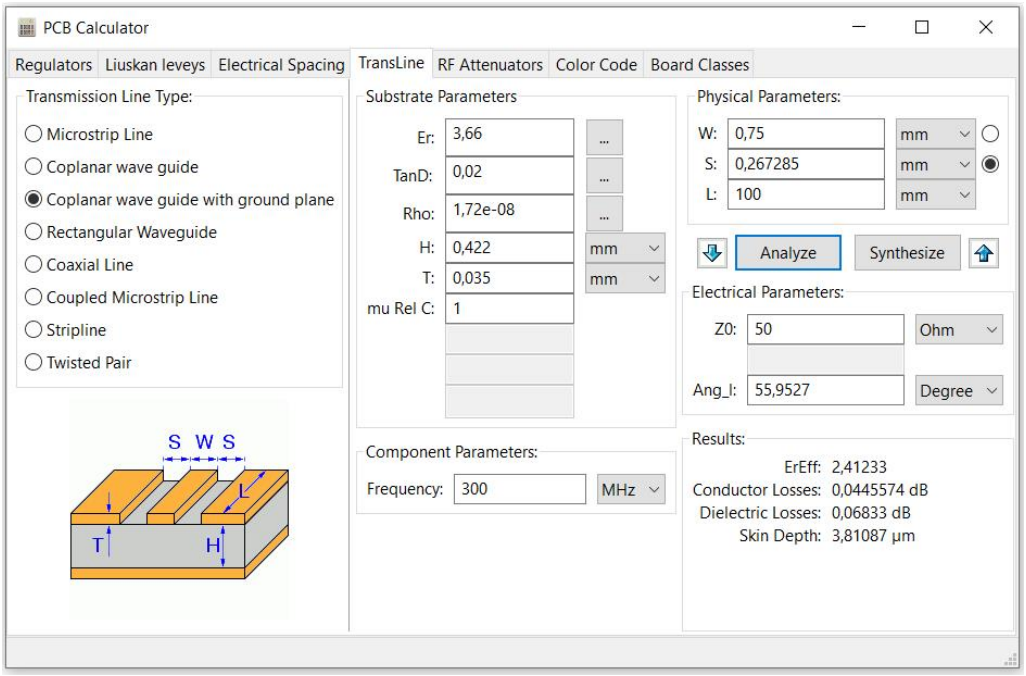

Figure 4.8. *KiCAD's PCB trace calculator.*

The RF signals are routed as coplanar on the top layer. The traces are matched to 50 ohm using KiCAD's PCB calculator. The simulation values are presented in Figure 4.8. Different PCB simulation softwares may result in a little bit different values for the trace synthesis, but in practice the impedance should be quite close $50\ \Omega$ with a small margin of error. The traces are designed as GCPW with width of the trace of 0.75 mm and the spacing of 0.267 mm. The distance H between signal and ground layer is 0.422 mm.

However, in the finalized product the distance H is increased form the initial value of 0.422 mm to 0.508 mm which will slightly increase the characteristic impedance to about $53\ \Omega$. This change is done in order to compensate for a soldermask attachment which typically decreases the TL's characteristic impedance by about 2–3 ohms [35].

The PCB traces and pads also require some coating, because the bare copper surfaces oxidize and deteriorate, resulting first decremented performance and finally making the whole circuit board unusable. The coating has two features, to protect the exposed copper planes and to provide a solderable surface for the component assembly.

For coating, electroless nickel immersion gold (ENIG) finish was chosen even though increasing slightly conductor losses due to nickel being less conductive than copper. It has excellent surface planarity which is ideal for soldering fine pitch components. Also, it is excellent for plating vias and exposed pads as it increases the heat transfer. Compared to other PCB coating processes ENIG finish is more expensive but it is restriction of hazardous substances (RoHS) compliant.

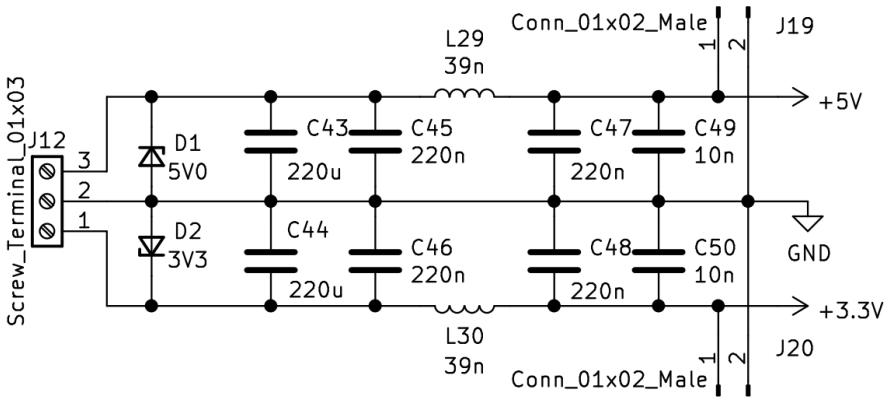

Figure 4.9. *DC power supply schematic.*

4.3.2 DC Power Supply

The DC input has three terminals: two supply voltages and one ground connection. Two separate V_{cc} values are needed, due to the components' 3.3V and 5.0V operating voltages. These voltages are routed in the third layer which is the dedicated power plane. All other layers have a ground plane. Both power supply lines have a corresponding Zener diode for voltage regulation which is combined with two input shunt capacitors (C), a series inductor (L) and two shunt output capacitors (C) forming a CLC filter to provide stable power supply [36]. The filter design uses both electrolytic and ceramic capacitors to filter out different frequencies [34, 36]. Also, light emitting diode (LED) indicators were added for cases, where lab's power supply front panel may not be visible. In addition, both lines have DC outputs as a placeholder with 1x02 male connectors. If they are left unused, some kind of protection is recommended to prevent accidental touching and short circuiting. All of the terminals and the pins have their descriptions written on the silk screen.

The power supply's KiCAD schematic is shown in Figure 4.9. The bias voltages for the PIN-diode attenuators are provided with a simple voltage divider design. The needed bias voltage is about 0.65–0.75 V [45] and applied for both branches. The bias voltage can be calculated by using the following equation:

$$V_{bias} = \frac{R_1}{R_1 + R_2} V_{cc}, \tag{4.3}$$

where $R_1 = 1\ \mathrm{k\Omega}$ and $R_2 = 5.6\ \mathrm{k\Omega}$ and V_{cc} is 5.0 V. Both of these resistors are replaceable if tuning is needed later. Also, voltage of the 5.0 V rail can be increased up to 5.1 V before the Zener diode starts conducting and working as a voltage regulator. This allows small bias voltage tuning without a need to replace the resistors. However, a small increase in the operating voltage does not harm any devices on the board.

4.3.3 EMC

Electromagnetic interference (EMI) can cause major issues in either PIN-diode control voltages or feedback signals if they are left unprotected. Also, every component on the PCB has to be connected to a ground plane or a point. It is not ideal to leave any pins floating which may cause weird device behavior when a terminal enters an undefined state. The feedback signals provide crucial information for the control board as it tunes the PIN-diode attenuators to achieve best possible cancellation. If there is interference or distortion in either in input or output feedback signals, the control board is unable to find the optimal weights values.

The PIN-diode control is not linear as it is shown in Section 4.2.3. Control voltage values can be divided into two different-sized margins, where the first margin is 0–2 V providing high amounts of attenuation from -40 dB to -5 dB. The second one is 2–20 V providing only a small amounts of attenuation from -5 dB to -3 dB. Especially, when operating with high attenuation values, even changes of few millivolts will drastically affect the cancellation performance as the amplitudes or the phases are no longer perfectly matched due to the EMI.

The separation of signal traces reduces emissions, cross-talk and noise. Two high-speed signals running in parallel create EMI through cross-talk, in which one trace influences the second trace through inductive and capacitive coupling, creating forward and backward current between the traces [38]. Using vias for RF or differential traces must be avoided as both the characteristic impedance and the length changes [36]. Cables carrying analog signals are extremely vulnerable to EMI as it can be coupled from nearby sources or cables. This is particular problem for high-frequency signals. Fortunately, shielding and connecting these cables to ground at the both ends reduces the total amount of EMI [36]. Thus, the canceller prefers certain types on cables or connectors, such as coaxial and SMA.

In order to reduce EMI, ground area should be maximized as much as possible within the PCB [36], which works well with the chosen coplanar transmission line structure. Split and hashed ground planes usually result in higher impedance levels so it is preferred to have minimum amount of openings in the ground planes as possible [36, 39].

4.3.4 Power and Thermal Analysis

All of the components introduce some power losses, which are typically presented in the datasheets. Power losses will cause unwanted effects in the circuit, such as heating of resistive components and dielectric losses. The extra heat generated by the components has to be dealt with. Otherwise, the overall performance will decrease as shown in Section 3.3. The following power and thermal analysis identifies possible issues and gives some

Type	Part name	Dissipated Power	Max Input Power [W]
Coupler: 30 dB	MBDA-30-451HP	0.034 W (0.15 dB)	200
SPDT Switch	TS7225FK	0.065 W (0.30 dB)	10
1st SP8T Switch	SKY13418-485LF	0.089 W (0.45 dB)	5.6
Cable loss	Longest, 6th cable	0.045 W (0.25 dB)	-
2nd SP8T Switch	SKY13418-485LF	0.075 W (0.45 dB)	5.6
90 Deg Hybrid pi	QCN-3+	0.046 W (0.30 dB)	15
PIN Diode (min)	BAP70Q-125	0.322 W (3.00 dB)	20
Power Combiner (max)	SYPS-2-52HP+	0.178 W (3.50 dB)	15
Coupler: 10 dB	SYBDC-10-13HP+	0.129 W (10.0 dB)	10

Table 4.2. *Power losses with 1 W of RF input power.*

insights while doing the measurements with the RF canceller board.

A worst-case scenario is used to estimate the total power dissipation in the canceller board by summing up all the component specific power dissipations caused by the insertion losses. The 30 dB input coupler has 0.15 dB insertion loss. A protection switch has 0.30 dB of losses. The delay switch has 0.45 dB of losses. The longest delay cable has 0.25 dB insertion loss at 400 MHz, the 90-degree hybrid has a typical insertion loss of 0.30 dB, a single PIN-diode attenuator can be tuned from 3 dB to 45 dB, the power combiner has 0.5 dB insertion loss with additional loss of 3 dB when the I- and Q-components are equal. When the TX power is 100 W and a 20 dB coupler is used at canceller input, in the worst case, 1 W of power is thus entering the RF input of the canceller. The dissipated power values are listed in Table 4.2.

The total dissipated power losses in the main RF line are about 1 W, but they do not take into account the 2 I/Q demodulators which together consume about 2 W of power. Also, the dissipated power in the RF traces is not included as it is considerably small compared to other losses. In addition, for most of components, the maximum internal dissipated power rating is not specified so they cannot be compared against the calculated values in Table 4.2.

Operating with a high RF input power is not recommended since the delay bank switches have maximum input power of 37.5 dBm or 5.6 watts [43]. Thus, they would be the first components to break as the RF input power increases. The amount of the power entering the canceller's RF input can be decreased by changing the external input coupler to one with higher coupling value. For example, a 20 dB input coupler would lower the input power to 1 watt and being more suitable for canceller operation. However, the input coupler cannot be changed arbitrarily but must be calculated relative to the available antenna isolation. Here, the selection of the 20 dB input coupler assumes 40 dB of antenna isolation.

V1	V2	Active RF path
0	1	All off
0	0	Input $\rightarrow$ RF1 (Output)
1	0	Input $\rightarrow$ RF2 (Ground)

Table 4.3. *TS7225FK SPDT switch truth table [42].*

Thermal vias allow heat transfer in a PCB. These vias are located under thermal or exposed pads which are the main heat transfer paths from SMD components, even though some power is dissipated through the plastic package. The quantity, proximity and position of thermal vias have a direct impact as they provide a large reduction in thermal resistance and improve heat dissipation at a faster rate. Thermal vias work with multilayer boards by connecting the different copper pours. [57, 58]

Thermal resistance is calculated as a temperature difference between two closed surfaces divided by the total heat flow between them. Using SMD components has some impact on reducing thermal resistance [58]. However, the total surface area and thickness of the copper on the PCB and the thickness and material have a greater effect [57]. In addition, simulation tools, such as Altium or Cadence, can be used to analyze the performance of components and to identify possible hot spots on the board.

Heat is more easily dissipated from larger surfaces and thicker materials, such as ground planes or heat sinks [57]. The bottom side of the RF canceller board has no component placements which allows for a possible heat sink attachment. The heat sink is probably not needed because the heat losses are currently relatively small and the board already has a large surface area. The six M3 mounting holes at the edges can be used to attach the heat sink. Only issue is the through-hole components whose pins extend to the bottom side.

4.3.5 Control Circuit Interface

The RF canceller board requires a separate board for adaptive control, since this canceller prototype does not include the control circuit. This subsection will provide the interface for the different control signals which are used for turning on/off the protection switches, selecting a delay line, tuning I- and Q-components' weights. For example, I and Q control values are difficult to find quickly with manual tuning, but can be a simple task for an algorithm. Also, keeping a track of the voltage combinations for delay line selection is easier to implement with a software. For testing purposes, the manual tuning is fine, but some kind of Matlab script is needed for the measurements in order to automate the process.

Delay Line ID	Cable ID	V1	V2	V3	Active RF path	Pin Number
1	PCB Trace	0	0	0	Ant-RF1	3
2	1	0	1	0	Ant-RF3	2
3	2	1	0	0	Ant-RF5	1
4	3	1	1	0	Ant-RF7	14
5	4	1	1	1	Ant-RF8	12
6	5	1	0	1	Ant-RF6	11
7	6	0	1	1	Ant-RF4	10
8	7	0	0	1	Ant-RF2	9

Table 4.4. *SKY13418-485LF SP8T RF switch truth table [43].*

While using the TS7225FK protection switch, its V_{DD} should be applied first before the control voltages or the RF input signal, otherwise it may damage the device. The switch is considered open if the input is connected to the output. Respectively, the switch is closed when the input is connected ground. Both V1 and V2 control pins have internal pull-downs to ground. The switch state is open at a start-up because both control voltages are grounded. The different states are explained in Table 4.3. If the all off state is not used, the switch is opened or closed by applying a single control voltage to pin V1 and pin V2 can be connected to the ground. Both TS7225FK switches have a 2x02 male pin-header connector on the board with description for each pins. The logic is provided with DC voltages where high = 3.3 V and low = 0 V.

SKY13418-485LF is the delay switch and its control voltages are V1, V2 and V3, where high = 1.8 V and low = 0 V. Any state other than those described in Table 4.4 will place the switch into an undefined state. An undefined state will not damage the device, but denies proper function [43]. The delay cables can be connected arbitrarily but there is a preferred cable configuration labeled on the silkscreen. If this configuration is used same control voltage combination can be applied to both switches. Otherwise, the user have to define the new port pair for a certain delay cable.

Each BAP70Q-125 PIN-diode attenuator requires control voltage V_{ctrl} ranging from 0 V to 20 V. These DC voltages are applied through coaxial cables and the input terminals are marked as "PIN-Diode Control n" on the canceller board where the n denotes the number. Control circuit's digital-to-analog converter (DAC) should be chosen so it has enough bits for a smooth voltage adjustment. The number of possible different output levels which DAC can generate is known as resolution. This is the minimum voltage step which can be generated and it is calculated by using the following equation:

$$Resolution = \frac{V_{out}}{2^N}, \tag{4.4}$$

where V_{out} is DAC's maximum output voltage and N is number of bits. For example, assume a 10 bit DAC and output voltage range from 0 V to 10 V. In this case, the step size or resolution is equal to $10/2^{10}$. This results about 10 mV as resolution of DAC which might be a too large step. The most used adjustment range would be somewhere around 1–5 V, while the minimum and maximum attenuations outside this range are used less. Using either a 12 or 14 bit DAC would be recommended based on the calculations and the PIN-diode measurements.

5. MEASUREMENTS AND RESULTS

In this chapter, measurement results for the built RF canceller board are presented and analyzed. First, the used measurement equipment is introduced and the different setups are briefly described. Different canceller parameters are measured as a prerequisite for the actual operation, since they should satisfy the design principles and prove that the canceller circuit works as intended. Finally, the cancellation capability is measured and the performance is analyzed. All measurements have been done in a closed environment, allowing the canceller's operation to be studied in more detail.

Section 5.1 presents the used setup and measurement devices. In Section 5.2, general parameters related to canceller operation are measured and studied such as power consumption, impedance matching, insertion losses in the main RF paths, signal delays through the canceller, switching speeds of RF switches, canceller's tuning range and filter response. Section 5.3 focuses on the actual analog cancellation where cancellation performance is first studied as function of input power. Followed by cancellation with a desired signal and evaluating how far this transmitter can still be detected.

5.1 Measurement Setup

Measurements have two major setups that utilize different measurement devices. The two most important devices are a vector signal transceiver (VST) PXIe-5645r from National Instruments and a vector network analyzer (VNA) PNA N5224B from Keysight. In addition, some general signal generators and oscilloscopes are used. The RF input signal is amplified by a power amplifier, which is ZHL-2-12+ from Mini-Circuits with a typical gain of 26 dB and maximum on input power of +10 dBm [59].

The chosen input coupler is model 4216-10 from company Narda-MITEQ with power handling of 5 watts, insertion losses of 1.2 dB and coupling of 10 dB. Utilization of the input coupler in measurements is important because the coupled port can be connected to the RX input of the canceller which emulates the self-interference. An attenuator can be added to the coupled port to adjust the power level of the self-interference at the RX input. Thus, the canceller is easy to test in the laboratory without antennas and does not require high transmission power despite emulating that. The ratio between transmit power and input power can be changed with the input coupler so that the input power of

the canceller remains constant. In general, the choice of the input coupler must satisfy the following condition:

$$Antenna\ isolation(dB) - S21(Canceller, min) > Input\ coupler(dB) \tag{5.1}$$

where the $S21(Canceller, min)$ is 18.4 dB. This condition is due to the fact that the power of the RF input signal must be higher than the power of the RX signal in order to match the signals' powers by attenuating the RF input signal since the analog canceller is unable to amplify the RF input signal.

For example, using 100 watts of transmission power with 40 dB of antenna isolation requires an input coupler with coupling less than 21.4 dB so a 20 dB coupler can be selected, and the canceller's input power would be 30 dBm or 1 W. Scaling the canceller to higher transmission powers works similarly. In case of the 1 kW of transmission power with 50 dB of antenna isolation, the input coupler is changed to 30 dB, and the RF input power remains constant at 1 W. A problem occurs when approaching 10 kW of transmission power because the antenna isolation might not exceed 50 dB which means that the input power of the canceller must be increased to 10 watts.

The RF canceller board has a total of eight delay lines. The internal delay is referred as the first delay line. It was only utilized during the delay measurements. All of the other measurement scenarios are done with the six delay cable configuration. In other words, delay lines 2–7 were active during the measurements as the internal delay was ignored and the ports for the 8th delay line were terminated. A new improved set of cables is designed in Table 3.1 as a specific for this RF canceller design. However, the measurements use the old delay cables that were originally designed for the article [30]. Their lengths are presented in the previous section in Table 4.1. The measurement devices and delays are connected to the RF canceller board via coaxial cables whose velocity factor is 0.66c resulting about 5 ns delay per one meter of cable.

5.2 Canceller Parameters

Power Consumption

The power consumption is measured when the RF signals are present in the circuit. The canceller board has two different supply voltages: 3.3 V and 5.0 V, which would draw about corresponding 10 mA and 340 mA currents. These estimates are based on component's datasheets [42, 43, 54]. This information will help to set current limits at laboratory power supply and can be used as a rough indicator if the RF canceller board works or not. Considerably low currents may indicate that some part of the circuit is not powered or working properly. On the other hand, very high current may occur due to a short circuit.

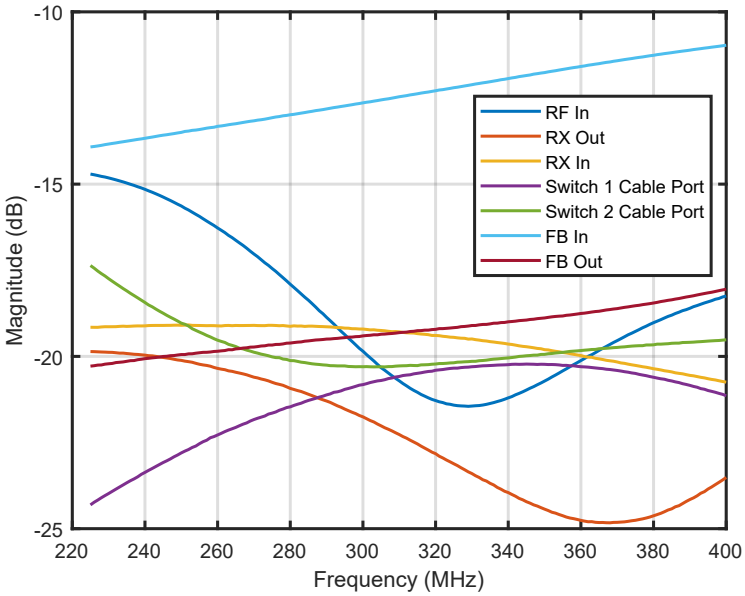

Figure 5.1. *Return loss: S11 versus frequency.*

The measured currents are 30 mA for 3.3 V and 356 mA for 5.0 V supply voltages, resulting a total current of about 390 mA. The current consumption is relatively higher than anticipated in the 3.3 V line because the SP8T switches tend to draw more current when the RF signal is applied. The estimation for 5.0 V line was quite accurate. The total power consumption can be calculated from the measured values and is approximated being about 1.9 W. Overall, the RF switches consume very small amount of the power compared to the two I/Q demodulators which use together about 1.6 W. The external control circuit will have its own power supply.

Impedance Matching and Losses

In order to improve the canceller's RF performance, all of the RF terminals should be matched close to $50\ \Omega$. This is proved by measuring the S11 parameter, also known as return loss, for each port while the other ports are terminated. All of the RF traces were designed to have a characteristic impedance of $50\ \Omega$ as calculated in Section 4.3.1. The measured return loss should be less than -10 dB over the entire frequency band. If the return loss is much higher than this, strong standing waves will be appearing, causing ripples in the frequency response. This ripple has a negative impact on cancellation performance because its effect cannot be cancelled. Also the ripple will affect the control circuit as it tries to estimate the SI and find optimal cancellation. The return loss measurement results are presented in Figure 5.1.

The results show that the return loss for each port is less than -10 dB, while most of them are even under -15 dB. Here, the feedback input (FB In) seems to have the weakest performance. The return loss of RF input port varies regarding to PIN-diodes' attenuation but it is always lower than the -10 dB marker in all of the cases. Low control voltages

from 0 V to 2 V typically weaken the return loss of RF input. Overall, these return loss measurements satisfy and prove the initial design principles.

The canceller's minimum insertion losses in the different RF paths are measured as the S21 parameter. The two main RF paths are from RF input to RX output and from RX input to RX output. During the measurement, PIN-diode attenuation is set to its minimum. This results in following values: $S21(RF_{In} \rightarrow RX_{Out}) = -18.4\ \mathrm{dB}$ and $S21(RX_{In} \rightarrow RX_{Out}) = -1.81\ \mathrm{dB}$. Both of these values correspond to insertion loss calculations in Section 4.3.4. The canceller's maximum attenuations are studied later in this section when analyzing the phase and amplitude tuning measurement results.

Delays and Switching Speed

It is important to know the total delay of the canceller board, while trying to match the canceller input signal and the SI in time domain. The total canceller delay is measured by using the implemented PCB trace on the canceller board and calculating the delay from RF input to RX output at 300 MHz yields about 3.96 ns. The delay slightly varies as function of frequency, while resulting in about 3.92 ns delay for 225 MHz and 4.01 ns delay for 400 MHz. The measured delay from RX input to RX output is about 0.93 ns.

The two vertical SMA connectors add some extra delay when a certain delay cable line is activated. The PCB trace lengths from the delay bank switch terminals to cable ports are compensated to match the length of the internal delay. However, the vertical SMA connectors add together about 0.125 ns extra delay to a cable line which is not compensated by the PCB layout design. The total delay with a cable can be estimated with the following equation:

$$Delay_{total} = Delay_{mainline} + Delay_{cable} + Delay_{connector} \tag{5.2}$$

While choosing the RF switches, switching speed, also referred as a total switching time, was a parameter of interest as discussed in Section 4.2.1. In practice, RF switches cannot react instantly because they are based on RF complementary metal oxide semiconductor (CMOS) technology. The reason is that a metal-oxide semiconductor field-effect transistor's (MOSFET) input capacitance has to be charged before its drain current starts conducting. Similarly, the switch off delay is caused by the discharge of the capacitance. [60]

It is beneficial to measure the switching speed for each type of RF switch, because it defines a time frame for opening and closing the switches. The information will be used later while designing control circuit and optimizing the adaptive control algorithms. Total switching speed is defined as a time it takes for a switch to connect the input signal to an another terminal and reaching its maximum value [40, 41]. It can be further divided into three time-related factors:

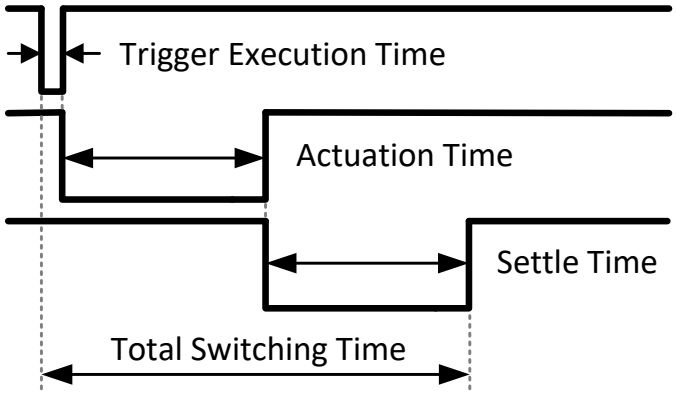

Figure 5.2. *Total switching time definition [41].*

1. *Trigger execution time*, also known as latency, is the time from a trigger command to a moment when a switch starts changing its state [41].
2. *Actuation time* is measured from beginning of the state change to a moment when contacts are fully opened or closed while also including the contact bounce [41].
3. *Settling time* is the period which it takes to stabilize the output signal once the switch is either opened or closed [41].

These three states are demonstrated in Figure 5.2. Adding them together will result the total switching time [41]. For example, the trigger command is an event when a control voltage is applied to the switch either via a PC input or manually operating the voltage source. The actuation time is defined here as the moment when output waveform can be distinguished from the noise floor. Usually, this will start slowly with only a tiny increase in the amplitude after each period and then rising fast. During the settling time, output voltage logarithmically approaches its final value. Settling is usually deemed to end when the output has reached a point where it is about 0.1 dB or 1% away from its final value [41]. Some manufacturers alternatively uses 90% of the final value as the limit [42, 43].

The measurements do not include the trigger execution time as it is quite difficult to be measured with an oscilloscope but this causes only a small error to the results. The final results can be rounded slightly upwards as a compensation. The measured switching speeds are shown in Table 5.1. TS7225FK's datasheet proposes a typical 0.7 μs of switching speed [42], while SKY13418-485LF's datasheet shows a typical 1.5 μs of switching speed [43]. The measured switching speed for TS7225FK was slightly over the value declared by the manufacturer. This is probably due to the fact that they specify total the switching time only up to 90% of the maximum value while the measurements assume 99%. The measured switching speed for SKY13814-485LF was under the datasheet's value because the real actuation time might be longer than measured as the exact starting moment is difficult to pin point. Datasheets do not specify separate values for either the actuation time or the settle time but only denote the total switching time for the com-

RF Switch	Actuation time [μs]	Settle time [μs]	Total Switching Time [μs]
TS7225FK	0.54	0.21	0.75
SKY13418-485LF	0.75	0.37	1.12

Table 5.1. *Switching speed measurement results.*

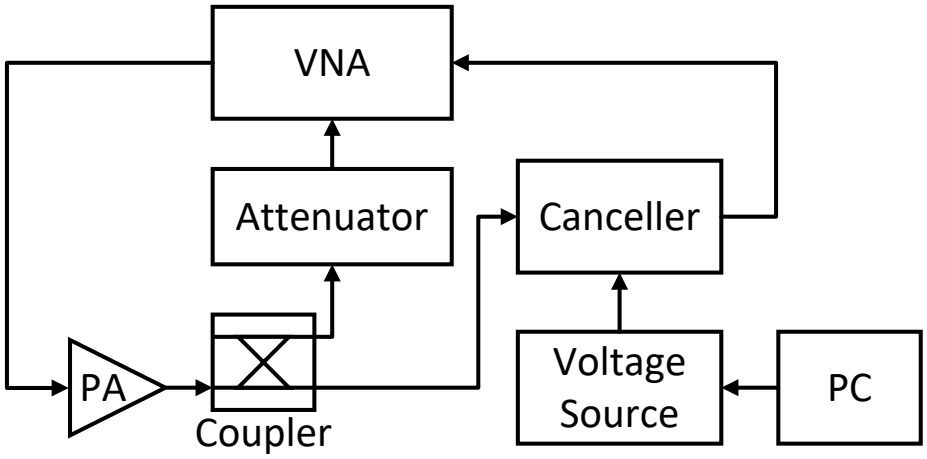

Figure 5.3. *Tuning range measurement setup using VNA.*

ponent. So the total switching times can be only compared. Overall, the measurement results line up well with the datasheet's typical values.

Canceller's tuning

The RF canceller's tuning range is measured to prove that the delay bank combined with the vector modulator can provide a full 360° phase coverage across the whole designed frequency band. Also, the measurement will show the maximum tuning range for the signal amplitude. This measurement utilized the VNA and a block diagram of the setup is shown in Figure 5.3, where the VNA's port 1 is connected to PA input, port 2 is connected to canceller's RX output and port 3 connected to coupler's coupled port via an attenuator. The measured coupler data from port 3 is later used to scale amplitudes accordingly because the PA will amplify the input signal. In reality, the canceller board attenuates the input signal and the effect of the PA has to be removed from the measurement results. The aim of the measurements is to study how the tuning of the RF canceller works with a high input power.

During the measurement, a single cable tuning range is swept over the whole frequency band from 225 MHz to 400 MHz. The control voltage V1 of the first PIN-diode attenuator is swept from 0 to 20 V while control voltage V2 of second PIN-diode attenuator is set to either 0 V or 20 V and then switched vice-versa. This will result in the outline for a single cable's tuning range. The outline is only measured because it will greatly reduce the total

measurement time as it is not needed to measure every single combination of V1 and V2 which is less interesting. The total measurement time would increase significantly if the whole region is measured accurately using a dense voltage grid. The used step size for the control voltages is 0.2 V from 0 V to 5 V and 1.0 V from 6 V to 20 V because the attenuation changes faster at low control voltages, so it is desired to measure the low voltages more accurately with a smaller step size. Measurement is repeated for each delay bank cable. The results in Figures 5.4, 5.5 and 5.6 are plotted on polar planes using a logarithmic scale.

The boundaries of each cable tuning range are drawn with a specific color to separate them from each other. All possible phases and amplitudes can be obtained within the boundaries of the tuning range of each cable. It demonstrates the overlap between adjacent delays and shows that there are different amount of overlap depending on which pair of cables is viewed at a certain frequency. It also illustrates how the tuning range of an individual cable rotates as the frequency changes. In some cases, the two cables will even overlap exactly like cables 1 and 6 at 300 MHz. In these cases, there is no practical significance of which one to choose. Typically, the edges of the adjustment range are avoided in order not to expose the canceller to non-linear operation. The middle section of the tuning range can be considered as a safe operation region.

By analyzing the measurement results on different frequencies, full phase coverage can be seen, except for 225 MHz where a small 5–6 degree gap appears due to the manufacturing errors in the old cables which were used in this measurement. This gap is between cables 1 and 6 as shown in Figure 5.4. The error in the cable lengths caused small phase shifts into opposite directions creating this gap. This is not seen as problem because the new designed cables will fix this gap. Also, the internal delay can be activated as it covers this gap perfectly.

The results also show the canceller's amplitude tuning range at different frequencies. The canceller's attenuation can be adjusted from -18.4 dB to -67.7 dB resulting a tuning range of 49.3 dB at 225 MHz. The amplitude tuning range decreases slightly as the frequency increases. For example, the tuning range is about 44.5 dB at 400 MHz. The amplitude control is not linear, as it changes really sharply at low control voltages, which reduces the control accuracy. Thus, it is generally preferred to change the canceller setup rather than attempting to operate with high attenuation values. The measured amplitude tuning ranges are similar to the previous PIN diode simulations and measurements in Section 4.2.3.

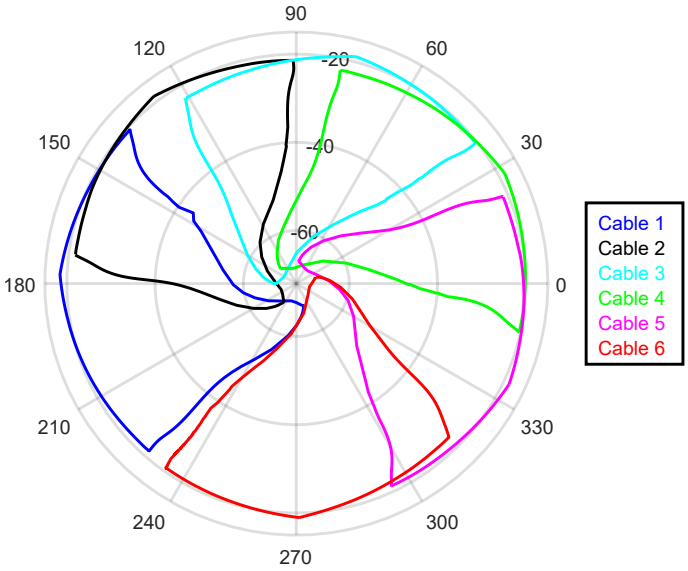

Figure 5.4. *PIN-diode attenuator tuning range at 225 MHz.*

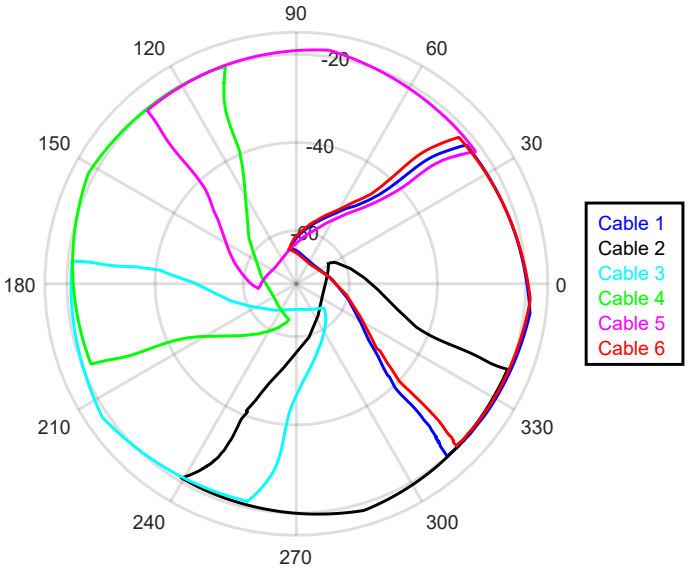

Figure 5.5. *PIN-diode attenuator tuning range at 300 MHz.*

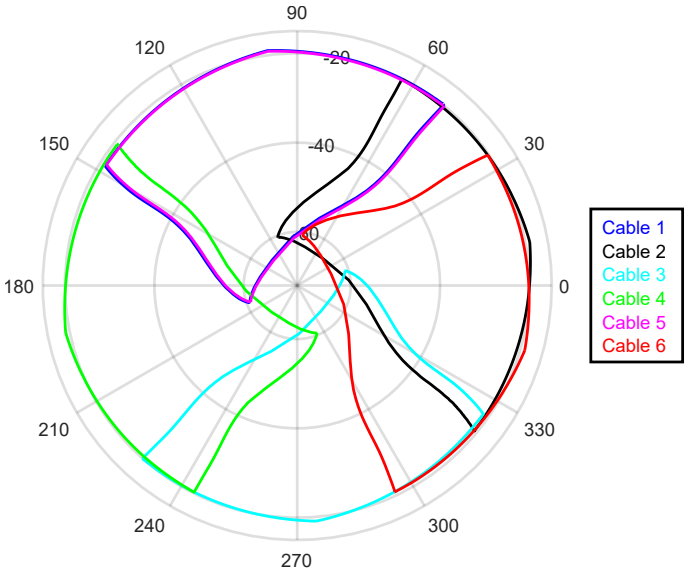

Figure 5.6. *PIN-diode attenuator tuning range at 400 MHz.*

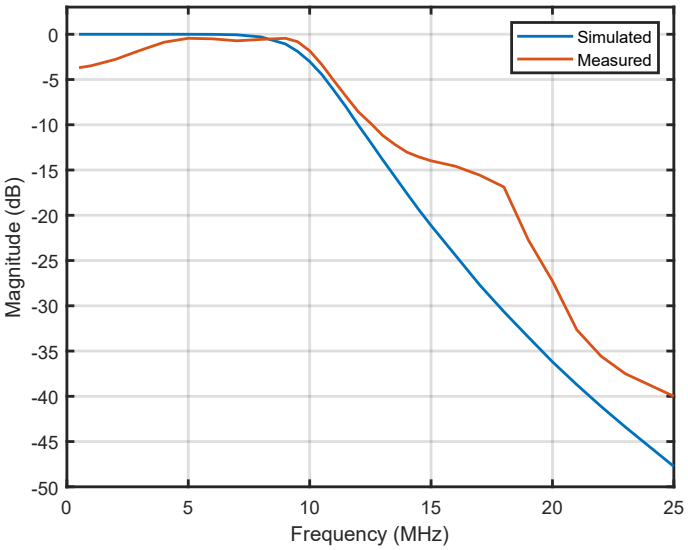

Figure 5.7. *Simulated and measured 10 MHz filter response.*

Filter Response

Both of the I/Q-demodulators have a 6th-order Butterworth low-pass filters with cut-off frequency of a 10 MHz. The filter response can be measured with a spectrum analyzer or a VNA, while the filter is connected between the probes. A problem is that the filter cannot be directly measured as it is in series with the I/Q demodulator. So the filter has to be measured by having a fixed signal at the I/Q demodulator input while changing the LO frequency according to (4.2) presented in Section 4.2.5. The output is measured with an oscilloscope while increasing the down-converted frequency. The output values are recorded until the signal reaches the noise floor so it cannot be no longer distinguished.

The measured frequency response is plotted based on the recorded values and analyzed to confirm the bandwidth, cutoff frequency, and ripple. Since the filter is designed as Butterworth, it should not have any ripple on in its passband [53]. The measured filter response is compared against the simulated filter response from ADS, and both of them are plotted on Figure 5.7.

The measured response differs from the simulated response as it does not decrease as smoothly as designed and the passband is narrower. This is probably due to the design of the filter layout which introduces some parasitic inductances and capacitances that slightly change the response of the filter. The measured cutoff frequency is about 10.2 MHz by following the -3 dB rule and resulting a passband of about 1.6–10.2 MHz. However, the measured filter so far works fine on the passband but may be re-tuned later if it causes issues for the feedback signals.

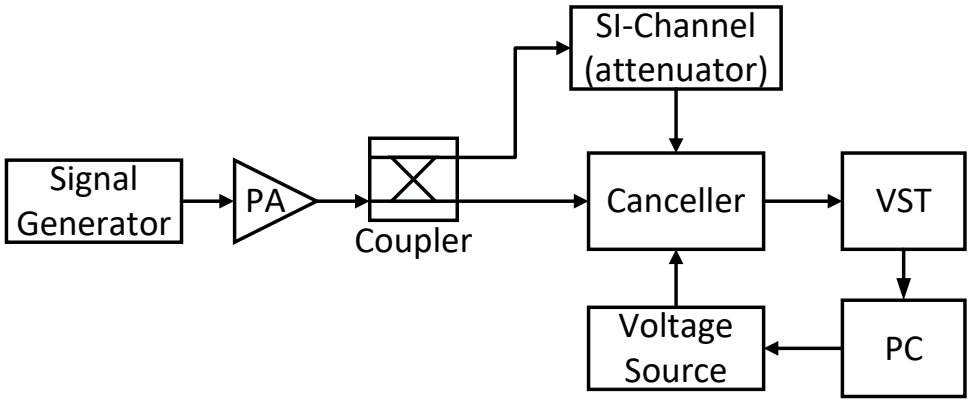

Figure 5.8. *RF canceller measurement block diagram.*

5.3 Analog Cancellation Performance

A block diagram of the cancellation measurement setup is presented in Figure 5.8. The initial RF input signal is created by a signal generator and amplified by the PA. The RF signal goes through the external input coupler to the canceller board's RF input port, while the coupled port is connected to the SI channel. The SI channel is an emulation of the actual antenna isolation and is implemented using an attenuator. Here, the total antenna isolation equals to the coupling value combined with the attenuation value. The SI channel is connected to canceller's RX input port. The canceller RX output is measured by the VST and the data is displayed on PC and analyzed by a user. The PC has a Matlab script that sets values for the voltage source as it controls both the delay bank and the vector modulator on the canceller board. This creates a feedback loop, and after few iterations the optimal cancellation should be established. The canceller has to tuned again if either the input signal's frequency or power has changed. In addition, any changes to the measurement setup will require re-tuning of the canceller. For example, replacing one RF cable will affect the phase difference, unless the new one has exactly the same length.

While measuring the cancellation, it is not needed to operate with 100 W of TX power. The power ratio between TX antenna and canceller RF input can be adjusted by changing the input coupler so that the RF input power remains constant regardless of TX power. It is not necessary to use the maximum transmission power under laboratory conditions, as it does not provide any benefit in terms of measurements.

Here, the PA's output power determines the maximum power that can be fed into canceller's RF input terminal. The canceller's maximum input power is measured by connecting the coupler output to the power analyzer, while the coupler input is fed by the PA. Thus, the small power losses in the cables and in the coupler are taken into account. During this measurement, it is noted that the output power starts saturating as the PA

input power is about to reach its maximum value. Based on this measurement, the maximum input power is about 28.20 dBm or 0.66 watts even though it was desired to have at least 30 dBm as maximum input power. It can be said that the PA is a bottleneck in this measurement setup. However, the cancellation performance measurements use the 28.20 dBm as the maximum available input power because a better PA was not available at the time of the measurements.

First, it is studied how the cancellation behaves as function of the input power. An initial guess is that, the cancellation should decrease as the input increases based on previous works studies in the research team and the analysis in Section 3.3. Additive white Gaussian noise (AWGN) is used as the input signal with bandwidth of 5 MHz to represents the self-interference. The cancellation performance is measured over three different bandwidths, which are 100 kHz, 500 kHz and 5 MHz around the center frequency. The first two bands represent the narrowband canceller performance for which this RF canceller was initially designed for while the 5 MHz band demonstrates the cancellation over wider bandwidth. The average power on a certain band is measured in two cases where the canceller is first inactive and then activated with an optimized cancellation. The total cancellation at the BW is equal to subtracting these values as shown in the following equation:

$$Cancellation = P_{avg,no\ cancellation} - P_{avg,cancellation} \tag{5.3}$$

The measurements are started with a low input power as it is a little bit easier to find the optimal cancellation that way for a certain frequency. The input power is increased until the maximum input power is reached and after each increment the cancellation is re-tuned, because the optimal I and Q weights slightly drift as the input power increases. Cancellation is optimized for the 100 kHz bandwidth which also results near the optimal cancellation for the 500 kHz bandwidth. No attempt has been made to optimize the cancellation for the 5 MHz band, but it has been measured with the same values as the two narrow bands. This measurement process is repeated for three different center frequencies which are 227.5 MHz, 300.0 MHz and 397.5 MHz as they show the cancellation performance at lower, middle and upper frequencies of the designed frequency range. The results are shown in Figure 5.9

The cancellation is measured with the input powers from 19.6 dBm to 28.2 dBm because the performance with high input powers is most essential for this analog canceller. It was of particular interest to study whether the effects of the non-linearity could be detected with this PA. It would have been possible that the non-linearity would have started to affect the cancellation from 30 dBm of input power and onwards. However, the non-linearity is present within the used input power range and is noted in the measurement results.

In Figure 5.9, the cancellation for the bandwidth of 100 kHz is plotted as a solid line, the bandwidth of 500 kHz is plotted as a dashed line and the wide bandwidth of 5 MHz

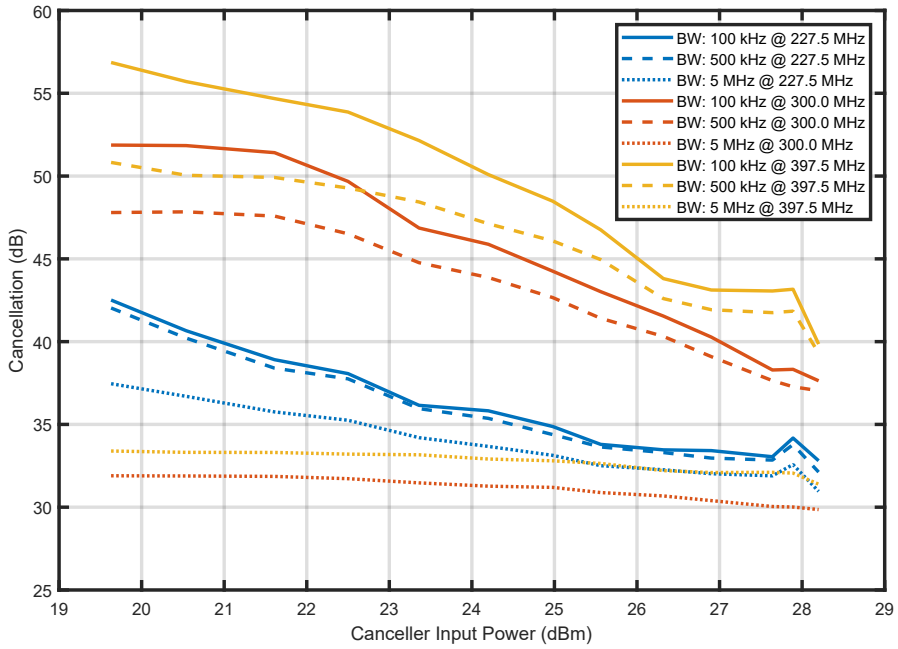

Figure 5.9. *Cancellation as function of canceller's input power.*

is plotted as a dotted line. The narrowband cancellation decreases in both cases at all frequencies as the input power increases. The 100 kHz cancellation is always better than the 500 kHz cancellation although the difference between them decreases as the input power increases, especially at low frequencies. The shape of the curves is very similar in the narrowband cases. The wideband cancellation remains constant for longer than narrowband cancellation and does not significantly deteriorate as the input power increases. However, a slight decreasing slope is noticeable for the wideband cancellation.

The narrowband measurements with the maximum input power result in about 32.8 dB of cancellation at 227.5 MHz, 37.6 dB of cancellation at 300.0 MHz and 39.9 dB of cancellation at 397.5 MHz. The effects of non-linearity are clearly seen when looking at input powers from 27 dBm to 28 dBm where the cancellation behaves strangely. Here, the cancellation may remain constant as the input power increases and momentarily even improve until it decreases steeply.

According to the measurement results, the canceller works best at higher frequencies while its performance is the weakest at the lower frequencies. An interesting observation is that wideband cancellation is increased when operating at low frequencies even though intuitively it would be assumed that the performance at 227.5 MHz would be the weakest of all there. This is partly due to the fact that the relative bandwidth is significantly higher at lower center frequencies than at higher center frequencies.

It can be noted that, at lower frequencies, the canceller behavior changes as it becomes more of wideband than narrowband canceller. This effect can seen on the 227.5 MHz

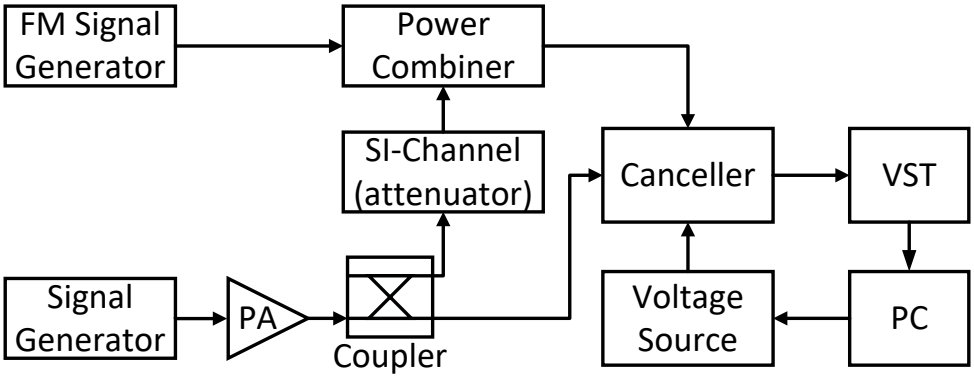

Figure 5.10. *Block diagram of cancellation measurement with FM signal.*

wideband graph as it follows shape of narrowband graphs and does not remain constant in the same way as for the 300.0 MHz and 397.5 MHz wide band cases. This may be due to the fact that the cut-off frequency of the PIN diodes increases with respect to the input power. The originally calculated 8 MHz cutoff frequency in Subsection 4.2.3 may have become closer to the lower operation frequency of the canceller, so that the requirement for the operation of the PIN diodes is no longer met. The requirement states that PIN diode's operation frequency must be considerably higher than the cut-off frequency.

Cancellation with a Desired Signal

The canceller performance can be also analyzed in a scenario where a narrowband signal is received while cancelling the interference at same frequency band. This new measurement setup includes few modifications to previous setup shown in Figure 5.8. Now, a second signal generator is added to create a narrowband frequency-modulated (FM) signal which simulates the desired signal. The SI and FM signals are combined by power combiner and then connected to the canceller's RX input terminal. The block diagram of this modified configuration is shown in Figure 5.10 and the measurement setup is shown in Figure 5.11.

The measurement is repeated on the same three center frequencies as used in the previous measurements. In the initial situation, the incoming desired signal is not detectable when the canceller is not active. The desired signal is hidden under the strong SI but will become distinguishable when the optimal cancellation is established. The power level of the desired FM signal is set so that the signal is about 3 decibels above the noise and it can be clearly distinguished from the RF spectrum when the RF canceller is active. The set power level of the FM signal describes its possible minimum value. The results are shown in Figure 5.12 where the left column provides a wide spectrum image and the right column shows a zoom on the desired signal.

The results are measured at maximum input power and are plotted as RF spectrum fig-

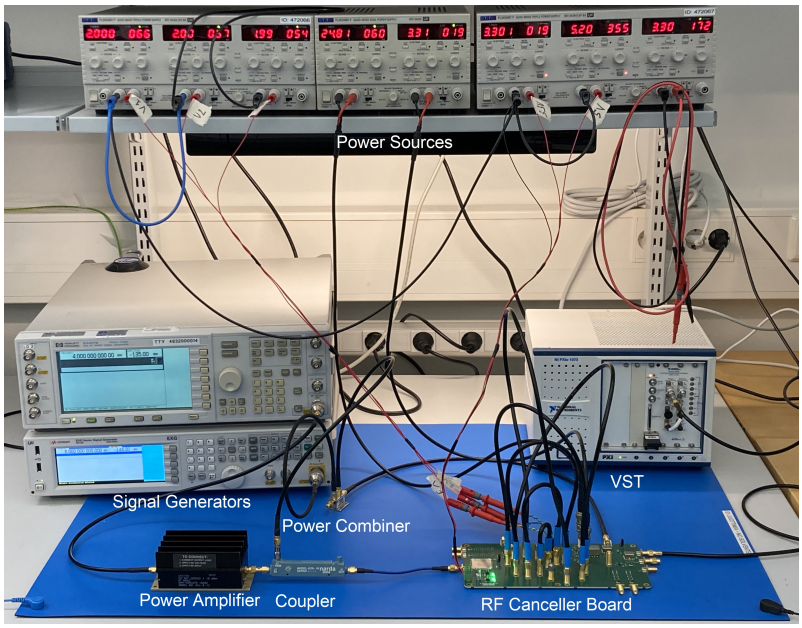

Figure 5.11. *Measurement setup.*

ures. The total cancellation can be roughly estimated by calculating the difference between the blue and orange curves over a given bandwidth. The blue curve represents the spectrum without cancellation and the orange curve shows the situation when the optimal cancellation is found. Based on these figures, the same conclusions can be drawn about the cancellation performance as from previous input power measurements. The zoomed figures shows the minimum received power for the received signal which are -35 dBm at 227.5 MHz, -40 dBm at 300.0 MHz and -50 dBm at 397.5 MHz.

If the different center frequencies are compared with each other, it is found that they form a slightly different spectrum figures after optimized cancellation is active. Both 227.5 MHz and 300.0 MHz form a spectrum figure which has stable signal level over entire the 5 MHz bandwidth and the desired signal is seen slightly above it. In case of 397.5 MHz, the signal level is no longer constant over the bandwidth but forms a valley shaped spectrum. The bottom of the valley is at the center frequency where the desired signal is also located. This shape occurs when cancellation works well and optimal weight values are found for both PIN diode attenuators and non-linearity does not significantly affect the cancellation.

The cancellation performance can be analyzed in practical systems and applications which are described in Section 2.4 by using the measurement results and utilizing link budget calculations. These calculations are intended to estimate the distance from which the incoming signal can still be detected according to measurement results. The received power P_{RX} can be calculated using following equation:

$$P_{RX} = P_{TX} + G - L_{FS} - L_{Misc}, \tag{5.4}$$

where P_{TX} is the transmitter output power, G includes all of the gains, such as TX and

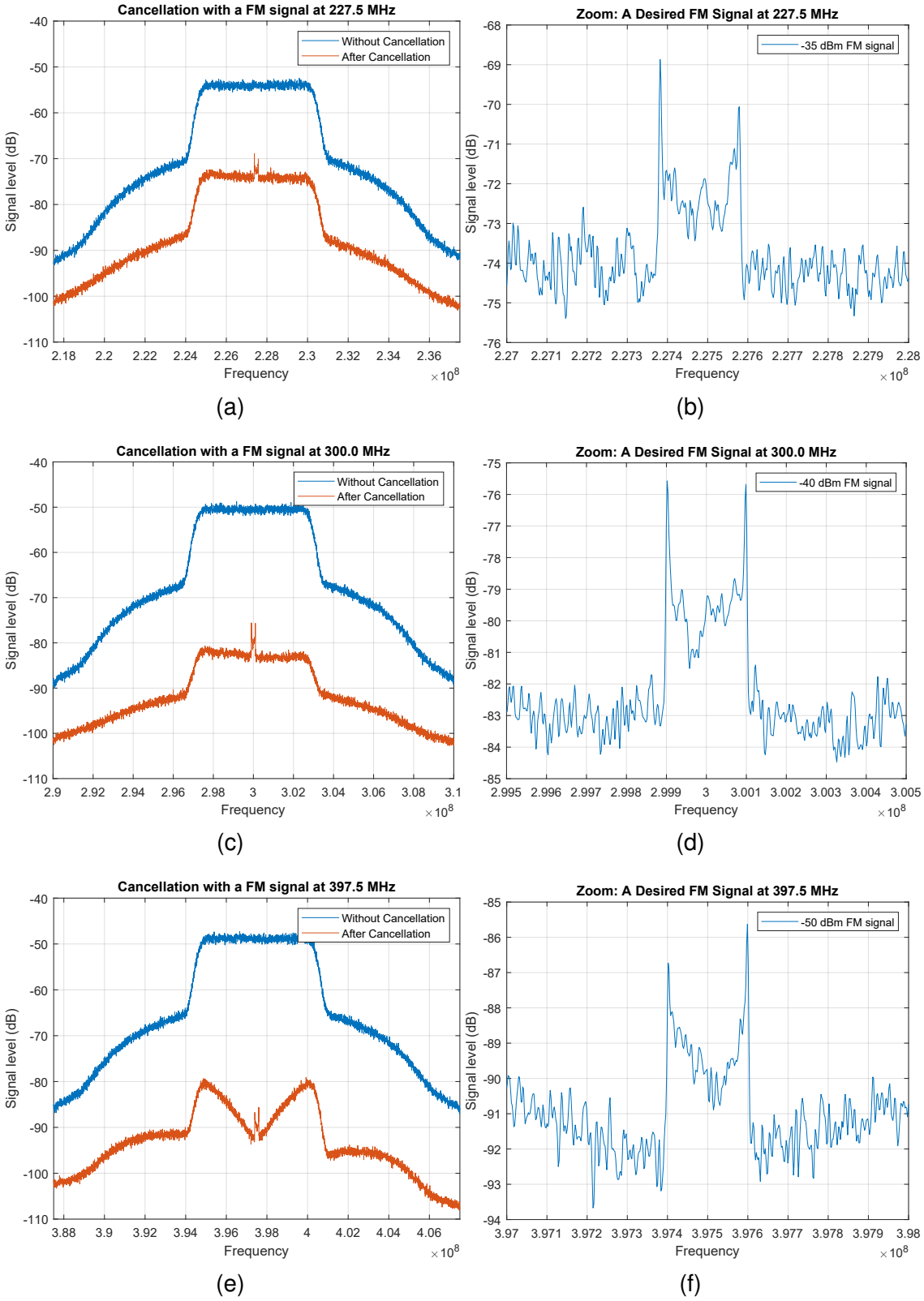

Figure 5.12. *Cancellation measurement with a desired FM signal.*

Frequency [MHz]	RX Signal Strength [dBm]	Detection Distance d [km]
225	-35	0.843
300	-40	1.124
400	-50	2.666

Table 5.2. *Link budget calculations.*

RX antenna gains, L_{FS} is the free space path loss (FSPL) and L_{Misc} includes all miscellaneous losses caused by cables, connectors, matching errors, polarization misalignment etc. The L_{FS} is expressed in dB scale using following equation:

$$L_{FS} = 20 \cdot \log_{10}\left(\frac{4\pi df}{c}\right), \tag{5.5}$$

where d is the distance between the RX and TX antennas, f is frequency and c is the speed of the light. Before solving for the distance, some assumptions have to be made about the system. Assume the following parameters: transmitter is an isotropic radiator with transmission power of 37 dBm, receiver antenna has gain of 8 dBi, miscellaneous losses are about 2 dB and received power P_{RX} is obtained from the measurement results presented in Figure 5.12.

The link budget calculations result in decent detection distances for all of the cases which are shown in Table 5.2. Here, the detection distance increases as a function of frequency resulting about 0.84 km at 225 MHz, 1.1 km at 300 MHz and 2.7 km at 400 MHz. This is a direct consequence of how well the RF canceller works at the specific frequency with a high input power. The canceller has weakest performance in low frequencies which was also proved by the previous cancellation versus input power measurements.

These distance calculations are only indicative results because a lot of different assumptions have to be made about the link system. Small changes in several parameters can significantly change the results in either direction. In addition, the FSPL assumes unobstructed terrain, but in reality there is likely to be some kind of vegetation between the transmitter and receiver that causes the incoming desired signal to attenuate even more. The two cancellation measurements can be combined to obtain detection distances as a function of input power. These results are illustrated in Figure 5.13.

Based on the graphs, it can be seen that the detection distance can be increased from few kilometers to several kilometers if the input power is reduced. At 400 MHz, distances of up to tens of kilometers can be reached. If the non-linearity were to be eliminated or its effects could be significantly reduced at the high input power, the analog RF canceller would work well on its own. In addition, these calculations show how an 8 dB improvement in antenna isolation would improve transmitter detection over a longer distance. It is

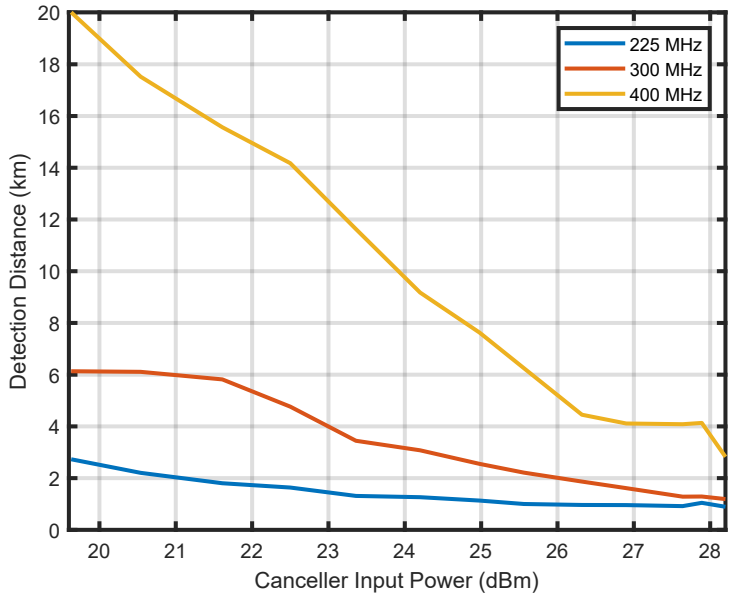

Figure 5.13. *Detection distance versus input power at three different frequencies.*

probably not necessary to use such a high canceller input power in practice as it was tested during the measurements. In addition, it should be noted that the measurements do not include any form of digital cancellation. So these detection distances are achieved by using only the analog RF canceller.

Most Recent Measurement Results

After the preliminary measurements presented in this chapter, this RF canceller prototype has been used in the article [61]. For the publication, most of the measurements were repeated and expanded to better cover the operation of the canceller. Based on the new measurements presented in [61], it can be shown that the phase coverage of the canceller also applies to high input powers and the cancellation could be significantly improved at all input powers and frequencies. It can be stated that the cancellation improved by an average of 5–10 dB, although the non-linearity is still not completely eliminated [61].

The main reasons for the improved results are the optimization of the measurement setup and more precise control of the variable attenuators. By slightly changing the measurement setup, it was to some extent possible to avoid non-linear operating regions that impaired cancellation. The changes were made mainly to the SI channel which now better emulates the ratio of the practical antenna isolation to the canceller input power. The changes resulted in improved cancellation of a few decibels, especially at high input powers. In addition, increasing the control voltage resolution from 10 mV to 1 mV allows for more accurate cancellation adjustment. This improves cancellation at low input powers where narrowband cancellation is significantly more sensitive to changes in control voltages. In reality, the canceller performs better than previously reported in this chapter.

6. CONCLUSION

In this thesis, a new high-power analog RF canceller architecture was developed for low frequencies with a narrow bandwidth and having a wide operation frequency range from 225 MHz to 400 MHz. The design is based on a new concept which has a delay bank in series with a vector modulator. The RF canceller has only one tap and it is designed for narrow-band signals. This canceller differs from previous designs because the structure enables the use of components with high power tolerances which allows the canceller to operate at higher input powers. Also, the low frequency band sets some limitations for the component choices. The RF canceller was built on a PCB, tested and measured. The purpose was to demonstrate the feasibility of the high-power RF canceller concept.

Analog cancellation is an important part of self-interference suppression along with antenna isolation and digital cancellation. The analog canceller prevents the saturation of the ADC and reduces the required dynamic range. The importance of utilizing all three methods is especially evident when the transmission power is high because none of the methods alone would be able to cancel the self-interference all the way down to the receiver noise floor.

Laboratory measurements show that the analog canceller circuit is capable of providing the full 360-degree vector modulation for the entire frequency range. The amplitude has about 40–50 dB tuning range with the PIN diode attenuators. The measurements result in about 30–40 dB of cancellation depending on the center frequency even though the high input power clearly impairs the cancellation performance as it was anticipated. Link budget calculations are applied to estimate the detection distance of a transmitter operating in the same frequency band while cancelling the self-interference. The transmitter produces a desired signal and is assumed to be an isotropic radiator with 5 watts of transmission power. The calculated detection distances for the incoming desired signals result in about 0.8 km at 225 MHz, 1.1 km at 300 MHz and 2.7 km at 400 MHz with the maximum available input power. Together with a digital canceller, the aforementioned detection distances can be greatly increased.

However, the non-linearity of the PIN diode attenuators proved to be a major issue for the RF canceller because their P1dB compression point drastically decreases with low control voltages. Thus, the attenuation range of the PIN diodes is limited because high

attenuations are obtained with low control voltages. This unwanted feature affects the cancellation performance when combined with the canceller's high input power. The components before the PIN diodes slightly attenuate the power of the input signal, but this is not sufficient. The problem is particularly evident at the edges of the tuning ranges, where either one control voltage or both of them are close to zero. This can be addressed by increasing the overlap of the delay cables and adding more delays, eliminating the need to operate at the edges of the control ranges.

The RF canceller is viable to be scaled up to 1 kW of transmission power by changing the external input coupler's coupling to 30 dB and assuming 50 dB of antenna isolation so that the canceller's input power remains constant. The current maximum input power for this canceller revision is about 1 W after which cancellation performance begins to drop drastically. The input power restriction is set mainly by the non-linear operation of the PIN-diode attenuators. The RF canceller board withstands input power up to 5 watts after which the first components begin to break down irreversibly.

So far, the canceller circuit has been adjusted manually which always requires a few iteration rounds to find the optimal cancellation. The next step in the canceller design will be the implementation of the control circuit and the development of adaptive control algorithms. Thus, it would be easier to demonstrate the performance of the RF canceller outdoors in the real operation environment. In addition, the canceller needs some kind of automated calibration system implemented in the control circuit.

Later, an improved version of the canceller could be built that would be smaller in size and more compact where the all of the delay lines would be implemented as PCB traces. This new version would take into better account of the non-linearity of the components. For example, by having two cascaded PIN diode attenuators a single attenuator does not need to provide high amount of attenuation and is less likely to suffer from non-linearity. Also, some of the previous component choices could be revised.

REFERENCES

[1] Kwak, J. W., Sim, M. S., Kang, I.-W., Park, J. and Chae, C.-B. Antenna/RF Design and Analog Self-Interference Cancellation. *Full-Duplex Communications for Future Wireless Networks*. Ed. by H. Alves, T. Riihonen and H. A. Suraweera. Singapore: Springer Singapore, 2020, pp. 39–60. ISBN: 978-981-15-2969-6. DOI: 10.1007/978-981-15-2969-6_2.

[2] Rosson, P., Dassonville, D., Popon, X. and Mayrargue, S. SDR based test bench to evaluate analog cancellation techniques for In-Band Full-Duplex transceiver. *2017 Fifth International Workshop on Cloud Technologies and Energy Efficiency in Mobile Communication Networks (CLEEN)* (2017), pp. 1–5. DOI: 10.23919/CLEEN.2017.8045911.

[3] Sabharwal, A., Schniter, P., Guo, D., Bliss, D. W., Rangarajan, S. and Wichman, R. In-Band Full-Duplex Wireless: Challenges and Opportunities. *IEEE Journal on Selected Areas in Communications* 32.9 (2014), pp. 1637–1652. DOI: 10.1109/JSAC.2014.2330193.

[4] Lajos Hanzo, J. B. and Ni, S. 3G, HSPA and FDD versus TDD Networking: Smart Antennas and Adaptive Modulation. Wiley-IEEE Press, 2008. ISBN: 978-0-470-75429-0.

[5] Kolodziej, K. E., Perry, B. T. and Herd, J. S. In-Band Full-Duplex Technology: Techniques and Systems Survey. *IEEE Transactions on Microwave Theory and Techniques* 67.7 (2019), pp. 3025–3041. DOI: 10.1109/TMTT.2019.2896561.

[6] Stutzmann, W. L. and Thiele, G. A. *Antenna Theory and Design*. Version 3rd ed. 2013. URL: http://www.eletrica.ufpr.br/armando/index_arquivos/Antenna_theory_and_design_Stutzman_Gary_Thiele%5C%20.pdf.

[7] Heino, M., Venkatasubramanian, S. N., Icheln, C. and Haneda, K. Design of Wavetraps for Isolation Improvement in Compact In-Band Full-Duplex Relay Antennas. *IEEE Transactions on Antennas and Propagation* 64.3 (2016), pp. 1061–1070. DOI: 10.1109/TAP.2015.2513081.

[8] Everett, E., Sahai, A. and Sabharwal, A. Passive Self-Interference Suppression for Full-Duplex Infrastructure Nodes. *IEEE Transactions on Wireless Communications* 13.2 (2014), pp. 680–694. DOI: 10.1109/TWC.2013.010214.130226.

[9] Iwamoto, K., Heino, M., Haneda, K. and Morikawa, H. Design of an Antenna Decoupling Structure for an Inband Full-Duplex Collinear Dipole Array. *IEEE Transactions on Antennas and Propagation* 66.7 (2018), pp. 3763–3768. DOI: 10.1109/TAP.2018.2835301.

[10] Valvo. *Application Note: ANV001, Circulator*. URL: https://valvo.com/wp-content/uploads/2017/12/CIRCULATOR.pdf (visited on 07/12/2021).

[11] Hassani, S. A., Lampu, V., Parashar, K., Anttila, L., Bourdoux, A., Liempd, B. v., Valkama, M., Horlin, F. and Pollin, S. In-Band Full-Duplex Radar-Communication System. *IEEE Systems Journal* 15.1 (2021), pp. 1086–1097. DOI: 10.1109/JSYST.2020.2992689.

[12] Laughlin, L., Beach, M. A., Morris, K. A. and Haine, J. L. Electrical balance duplexing for small form factor realization of in-band full duplex. *IEEE Communications Magazine* 53.5 (2015), pp. 102–110. DOI: 10.1109/MCOM.2015.7105648.

[13] Couraud, B., Vauche, R., Daskalakis, S. N., Flynn, D., Deleruyelle, T., Kussener, E. and Assimonis, S. Internet of Things: A Review on Theory Based Impedance Matching Techniques for Energy Efficient RF Systems. *Journal of Low Power Electronics and Applications* 11 (Mar. 2021), p. 16. DOI: 10.3390/jlpea11020016.

[14] Tamminen, J., Turunen, M., Korpi, D., Huusari, T., Choi, Y.-S., Talwar, S. and Valkama, M. Digitally-controlled RF self-interference canceller for full-duplex radios. *2016 24th European Signal Processing Conference (EUSIPCO)*. 2016, pp. 783–787. DOI: 10.1109/EUSIPCO.2016.7760355.

[15] Huusari, T., Choi, Y.-S., Liikkanen, P., Korpi, D., Talwar, S. and Valkama, M. Wideband Self-Adaptive RF Cancellation Circuit for Full-Duplex Radio: Operating Principle and Measurements. *2015 IEEE 81st Vehicular Technology Conference (VTC Spring)*. 2015, pp. 1–7. DOI: 10.1109/VTCSpring.2015.7146163.

[16] Ahmed, E. and Eltawil, A. M. All-Digital Self-Interference Cancellation Technique for Full-Duplex Systems. *IEEE Transactions on Wireless Communications* 14.7 (2015), pp. 3519–3532. DOI: 10.1109/TWC.2015.2407876.

[17] Freeman, R. L. *Radio System Design for Telecommunications 3rd Edition*. Wiley-IEEE Press, 2007. ISBN: 9780471757139.

[18] Riihonen, T., Korpi, D., Turunen, M. and Valkama, M. Full-duplex radio technology for simultaneously detecting and preventing improvised explosive device activation. *2018 International Conference on Military Communications and Information Systems (ICMCIS)*. 2018, pp. 1–4. DOI: 10.1109/ICMCIS.2018.8398707.

[19] Riihonen, T., Korpi, D., Turunen, M., Peltola, T., Saikanmäki, J., Valkama, M. and Wichman, R. Tactical Communication Link Under Joint Jamming and Interception by Same-Frequency Simultaneous Transmit and Receive Radio. *MILCOM 2018 - 2018 IEEE Military Communications Conference (MILCOM)*. 2018, pp. 1–5. DOI: 10.1109/MILCOM.2018.8599793.

[20] Riihonen, T., Korpi, D., Turunen, M., Peltola, T., Saikanmäki, J., Valkama, M. and Wichman, R. Military Full-Duplex Radio Shield for Protection Against Adversary Receivers. *2019 International Conference on Military Communications and Information Systems (ICMCIS)*. 2019, pp. 1–6. DOI: 10.1109/ICMCIS.2019.8842696.

[21] Pärlin, K., Riihonen, T., Karm, G. and Turunen, M. Jamming and Classification of Drones Using Full-Duplex Radios and Deep Learning. *2020 IEEE 31st Annual International Symposium on Personal, Indoor and Mobile Radio Communications*. 2020, pp. 1–5. DOI: 10.1109/PIMRC48278.2020.9217351.

[22] Adrat, M., Keller, R., Tschauner, M., Wilden, S., Le Nir, V., Riihonen, T., Bowyer, M. and Pärlin, K. Full-Duplex Radio – Increasing the Spectral Efficiency for Military Applications. *2019 International Conference on Military Communications and Information Systems (ICMCIS)*. 2019, pp. 1–5. DOI: 10.1109/ICMCIS.2019.8842748.

[23] Yener, A. and Ulukus, S. Wireless Physical-Layer Security: Lessons Learned From Information Theory. *Proceedings of the IEEE* 103.10 (2015), pp. 1814–1825. DOI: 10.1109/JPROC.2015.2459592.

[24] Anajemba, J. H., Tang, Y., Iwendi, C., Ohwoekevwo, A., Srivastava, G. and Jo, O. Realizing Efficient Security and Privacy in IoT Networks. *Sensors* 20.9 (2020). ISSN: 1424-8220. DOI: 10.3390/s20092609.

[25] Pinto, P. C., Barros, J. and Win, M. Z. Wireless physical-layer security: The case of colluding eavesdroppers. *2009 IEEE International Symposium on Information Theory*. 2009, pp. 2442–2446. DOI: 10.1109/ISIT.2009.5206050.

[26] Kolodziej, K. E., Cookson, A. U. and Perry, B. T. RF Canceller Tuning Acceleration Using Neural Network Machine Learning for In-Band Full-Duplex Systems. *IEEE Open Journal of the Communications Society* 2 (2021), pp. 1158–1170. DOI: 10.1109/OJCOMS.2021.3080618.

[27] Bharadia, D., McMilin, E. and Katti, S. Full Duplex Radios. *SIGCOMM Comput. Commun. Rev.* 43.4 (Aug. 2013), pp. 375–386. ISSN: 0146-4833. DOI: 10.1145/2534169.2486033.

[28] Duarte, M. and Sabharwal, A. Full-duplex wireless communications using off-the-shelf radios: Feasibility and first results. *2010 Conference Record of the Forty Fourth Asilomar Conference on Signals, Systems and Computers* (2010), pp. 1558–1562. DOI: 10.1109/ACSSC.2010.5757799.

[29] Duarte, M., Dick, C. and Sabharwal, A. Experiment-Driven Characterization of Full-Duplex Wireless Systems. *IEEE Transactions on Wireless Communications* 11.12 (2012), pp. 4296–4307. DOI: 10.1109/TWC.2012.102612.111278.

[30] Heino, M., Turunen, M., Vuorenmaa, M. and Riihonen, T. Design of RF Self-interference Cancellation Circuit for 100-W Full-Duplex Radio at 225–400 MHz. *2021 International Conference on Military Communication and Information Systems (ICMCIS)*. 2021, pp. 1–6. DOI: 10.1109/ICMCIS52405.2021.9486417.

[31] Pro-Power. *RG58 Coaxial Cable*. RG-58. Rev. V1.2. URL: http://www.farnell.com/datasheets/2095749.pdf.

[32] Hewlett-Packard. *A Low-Cost Surface Mount PIN Diode Attenuator*. Version Application Note 1048. URL: http://www.hp.woodshot.com/hprfhelp/4_downld/lit/diodelit/an1048.pdff.

[33] *Quad PIN Diode Attenuator*. MA4P7455-1225. Rev. V2. Macom. URL: https://cdn.macom.com/datasheets/MA4P7455-1225.pdf.

[34] Pozar, D. M. *Microwave Engineering, 4th Edition*. 2011. ISBN: 978-0-470-63155-3.

[35] John Bushie, A. V. *The Printed Circuit Designer's Guide to Fundamentals of RF / Microwave PCBs*. Version ISBN: 978-0-9998648-0-7. 2018. URL: https://www.ieee.li/pdf/essay/rf-microwave_pcb_fundamentals.pdf.

[36] Ott, H. W. *Noise Reduction Techniques in Electronic Systems*. Version 2nd ed. 1988. URL: https://commons.princeton.edu/motorcycledesign/wp-content/uploads/sites/70/2019/08/otto_1988_noisereduction.pdf.

[37] Chan, K.-C. *Technical Document: IP3 and intermodulation guide*. Maxim Integrated. June 29, 2012. URL: https://www.maximintegrated.com/en/design/technical-documents/tutorials/5/5429.html (visited on 11/23/2021).

[38] Carr, J. *The Technician's EMI Handbook, First Edition*. Newnes, 2000. ISBN: 978-0080518589.

[39] Clyde Coombs, H. H. *Printed Circuits Handbook, Seventh Edition*. McGraw-Hill Professional, 2015. ISBN: 9780071833950.

[40] Technologies, A. *Switching Handbook, A Guide to Signal Switching in Automated Test Systems*. 2007. URL: https://archive.eetasia.com/www.eetasia.com/ARTICLES/2007JUL/PDF/EEOL_2007JUL03_NETD_POW_AN.pdf.

[41] Keithley Instruments, I. *Power Handling Capability of Electromechanical Switches*. Version Fourth Edition. 2001. URL: https://assets.testequity.com/te1/Documents/pdf/keithley/switching-handbook.pdf.

[42] *10W CW GaN Broadband RF Switch SPDT*. TS7225FK. Rev. 1.7. Tagore Technology. 2020. URL: http://www.tagoretech.com/PartNumber/ts7225fk.pdf.

[43] *0.1 to 3.8 GHz SP8T Antenna Switch*. SKY13418-485LF. Skyworks Solutions Inc. 2016. URL: https://pdf1.alldatasheet.com/datasheet-pdf/view/952382/SKYWORKS/SKY13418-485LF.html.

[44] *Power Splitter/Combiner*. QCN-3+. Rev. E. Mini-Circuits. URL: https://www.minicircuits.com/pdfs/QCN-3+.pdf.

[45] *Quad PIN diode attenuator*. BAP70Q,125. NXP Semiconductors. 2018. URL: https://www.nxp.com/docs/en/data-sheet/BAP70Q.pdf.

[46] *Carrier Lifetime and Forward Resistance in RF PIN-Diodes*. Application Note No. 034. Rev. 2.0, Oct. 2006. Infineon. URL: https://www.infineon.com/dgdl/AN034.pdf?fileId=db3a304313d846880113de8d362503df.

[47] Jamil, M. and Md Yusof, N. N. A Review Of Wilkinson Power Divider As A Splitter/Combiner Based On Method, Design And Technology. Nov. 2014.

[48] *Power Splitter/Combiner*. SYPS-2-52HP+. Rev. B. Mini-Circuits. URL: https://www.minicircuits.com/pdfs/SYPS-2-52HP+.pdf.

[49] Mini-Circuits. *Application Note: Directional Couplers*. Sept. 8, 1999. URL: https://www.minicircuits.com/app/COUP7-2.pdf.

[50] Sengal, U. *Directional Couplers: Their Operation and Application*. Mini-Circuits, Application Note. July 12, 2022. URL: https://blog.minicircuits.com/directional-couplers-their-operation-and-application/.

[51] *DC Pass, High Power Bi-Directional Coupler*. MBDA-30-451HP. Rev. B. Mini-Circuits. URL: https://www.minicircuits.com/pdfs/MBDA-30-451HP.pdf.

[52] *Bi-Directional Coupler*. SYBDC-10-13HP+. Mini-Circuits. URL: https://www.minicircuits.com/pdfs/SYBDC-10-13HP+.pdf.

[53] Winder, S. *Analog and Digital Filter Design, 2nd Edition*. Newnes, 2002. ISBN: 978-0750675475.

[54] *Quadrature Demodulator*. ADL5387. Rev. C. Analog Devices. URL: https://www.analog.com/media/en/technical-documentation/data-sheets/ADL5387.pdf.

[55] *RF Transformer*. TCM9-1+. Rev. F. Mini-Circuits. URL: https://www.minicircuits.com/pdfs/TCM9-1+.pdf.

[56] John Coonrod, R. C. *Comparing PCBs for Microstrip and Grounded Coplanar Waveguide Circuits*. Apr. 4, 2020. URL: https://rogerscorp.com/blog/2020/comparing-pcbs-for-microstrip-and-grounded-coplanar-waveguide-circuits (visited on 10/11/2021).

[57] Remsburg, R. Introduction to Thermal Design of Electronic Equipment. *Advanced Thermal Design of Electronic Equipment*. Boston, MA: Springer US, 1998, pp. 1–20. ISBN: 978-1-4419-8509-5. DOI: 10.1007/978-1-4419-8509-5_1.

[58] Cadence. *Thermal Vias for Circuit Board Heat Management: Techniques and Tips*. 2019. URL: https://resources.pcb.cadence.com/blog/2019-thermal-vias-for-circuit-board-heat-management-techniques-and-tips (visited on 10/11/2021).

[59] *Power Amplifier*. ZHL-2-12+. Rev. ORM153516. Mini-Circuits. URL: https://www.minicircuits.com/pdfs/ZHL-2-12+.pdf.

[60] Razavi, B. *Fundamentals of Microelectronics, Second Edition*. Wiley, 2013. ISBN: 9781118156322.

[61] Vuorenmaa, M., Heino, M., Turunen, M. and Riihonen, T. RF Self-interference Canceller Prototype for 100-W Full-Duplex Operation at 225–400 MHz. *2022 International Conference on Military Communication and Information Systems (ICMCIS)*. 2022.